Supporting Information

O'Loughlin et al. 10.1073/pnas.1205130109

SI Text

After the detailed data descriptions, we present results for robustness tests that use spatial (country) and temporal (5-y periods) subsets of the East African data. We also present model modifications based on robustness testing of the effects of extreme climate conditions, growing season time periods, interaction terms, and alternative specifications of the dependent variable. All modeling includes year and country fixed effects and grid cell clustered SEs. The final set of models replaces country fixed effects with grid cell fixed effects.

I. Detailed Data Description. We have chosen the study area and time period for several reasons, including the degree to which our findings may be generalized to sub-Saharan Africa, and we recognized the availability of the necessary social, political, and climate data. First, 1990 has the benefit of representing the beginning of the post-Cold War contemporary world order. Material support for proxy actors coming from the Soviet Union and the United States profoundly influenced the political atmosphere, especially conflict dynamics, in many sub-Saharan African states between independence and 1990. Any findings gleaned from these earlier geopolitical realities would need to be applied cautiously to the current political climate, where such extensive external support is now generally absent. Second, empirical data for sub-Saharan Africa are notoriously undependable (or missing) during the earlier years of independence beginning in the early 1960s. By focusing on the period 1990–2009, we have access to more reliable data for social and political controls (e.g., governance type, socioeconomic status, and spatially disaggregated population data). Furthermore, the media-reported conflict events that we use have had more consistent and thorough coverage in the last two decades than during previous time periods. Third, the regions within the study area have exhibited a range of experiences with war and political violence, ranging from Tanzania (relatively calm) to northern Uganda (far more unstable). This wide representation of classifications of instability means that our study applies not only to already war-torn areas (a criticism of more classical work in the environmental security literature). Fourth, with regard to physical geography, our study area includes a wide range of climatic and meteorological zones. Variation for these underlying conditions allows us to analyze semiarid regions, which have been the focus of much previous work, but also extend to districts with other ecological characteristics (mountainous areas, rainforest, etc.). Fifth, we also have a relatively high degree of geographic variation with respect to control variables (e.g., population, socioeconomic status, and regime type).

Table S1 presents summary statistics for all of the variables used in the modeling.

a. Conflict data. The Armed Conflict Location and Event Dataset project (ACLED) codes media-reported conflict data (1). The existing database covers the period from 1997 to 2009 for most African countries, and we extended it back to 1990 for our set of nine East African states and bordering countries (Fig. S1). Much of the existing research on climate–conflict relationships relies on country-level data (2); however, their use is problematic, because conflict processes are typically unevenly distributed across the provinces or regions of a country. An especially egregious assumption of intracountry regional parity in violence yields assignment to large countries (e.g., Tanzania or Ethiopia) of a single binary measure of war or peace for each time period under study. The ACLED data are georeferenced with latitude and longitude coordinates, allowing for analysis of localized conflict within a country's borders. Compared with other datasets with high battle death thresholds, such as Correlates of War (threshold of 1,000 battle deaths/y) (3) or the Uppsala Conflict Data Program and Peace Research Institute Oslo (UCDP/PRIO; threshold of 25 battle deaths/y), the criteria for including violence in the ACLED data are relaxed (4). The number of deaths or amount of property damage associated with violence was not recorded in ACLED because of unreliable data reporting in news outlets. Furthermore, setting a fixed death threshold often does not make sense, because conflict emerging in the face of ecological stress might include small-scale skirmishes resulting in few deaths or injuries. The Correlates of War and UCDP/PRIO data record conflict only where it takes place between the government of an internationally recognized state and a cohesive rebel group. For our purposes, we identify and code violence that is not perpetrated by organized rebels or government forces; conflict often takes place between two nonstate actors, such as communal groups. Another data collection project, the Social Conflict in Africa Database, rejects a government–rebel and battle–threshold definition of conflict and insecurity but includes only conflict events that are more social or institutional in character; thus, it underreports the kind of violence that could result from ecological stress (5).

For our study area and time period, the raw data include 16,359 events. By type, the numbers of events are battle–government regains territory (359), battle–no change of territory (7,998), battle–rebel control of territory (550), riots/protests (1,359), and violence against civilians (6,093). Data are gathered from online sources, such as Lexis-Nexis and Factiva, as well as other sources, such as African Contemporary Record and African Research Bulletin. The precise date and location of every conflict event are recorded as well as the actors involved in the event and the type of conflict (battle, riots, etc.) that occurred. Both the temporal and spatial dimensions of the data have precision codes that indicate levels of (un)certainty. An exact location (e.g., town, village, or city) is coded as geoprecision level 1, a locality level estimate (e.g., a relatively fine resolution administrative unit such as district) is level 2, and a larger administrative unit (e.g., province) is level 3. Events geolocated at geoprecision level 3 are excluded from our analysis. For temporal precision, the exact date is coded as one, uncertainty within 1 wk is coded as two, and monthly precision is coded as three. We tested the model on data for one event type subset (the combined riots/protests and violence against civilians data) but with no noteworthy change on the core findings (see robustness checks below). Events taking place over 2 or more d are coded as individual consecutive entries rather than a date range, which is the method used by other projects.

Fig. S2 illustrates the distribution of violence over time and by type for each country in the study area. Certain spikes are evident, such as the violence that took place in Somalia during the last several years, from 2000 to 2004 in Burundi, the Ethiopia–Eritrea border wars in 1998–2001, and Lord's Resistance Army-related violence in northern Uganda. The large spike in Kenya reflects postelection violence, which was well-reported in the media. Although the spike in the spring of 1994 in Rwanda reflects the country's genocide, the number of events is not proportional to the enormous casualties (over 800,000), because the huge scale of the killings was not reported as clearly defined and discrete events.

b. Climate data. Precipitation. We use the 6-mo standard precipitation index (SPI6) to compare the most recent 6-mo precipitation record with the long-term distribution for the same season. The SPI for a given month and year depends on the chosen time scale. For example, the 6-mo measure, SPI6, compares the precipitation for

the past 6 mo with the average for the same interval over the years of record. Thus, SPI6 for June of 1990 compares the precipitation for January through June of 1990 with the historical average since 1949 for those same 6 mo.

Deviation in rainfall is one of the primary observable effects of climate change and variability, and most studies on the possible relationship of conflict to climate have used precipitation directly or indirectly in the analysis (6–9). Our precipitation and temperature data (1949–2009) are aggregated from the original University of East Anglia Climate Research Unit monthly 0.5° × 0.5°-grids Climate Research Unit database (10) to our study unit of analysis (1° × 1° grids) using local area averaging, which accounts for the fractional contributions of the high-resolution grid cells to each low-resolution grid cell.

We compared current precipitation to the long-term precipitation distribution parameterized using an incomplete γ-distribution (11). The current precipitation value is then converted to the standard normal distribution to aid interpretation between different climate zones. The SPI is the universal meteorological drought index recommended to the World Meteorological Organization by the Interregional Workshop on Indices and Early Warning Systems for drought (12). Although the Palmer Drought Severity Index is commonly used in the United States, it performs poorly in semiarid regions and regions with complex terrain, such as East Africa (13). The 6-mo SPI was chosen for this study, because it indicates medium-term trends in precipitation and provides information on the time scale of the growing season. It may also be related to anomalous stream flows and reservoir levels.

A drought period is defined when the SPI is negative and reaches a threshold value of −1.0 or less, whereas wet periods are defined for SPI ≥ 1.0. The SPI values are typically grouped into seven categories: ≥2.00 as extremely wet, 1.50–1.99 as severely wet, 1.00–1.49 as moderately wet, −0.99 to 0.99 as near normal, −1.00 to −1.49 as moderately dry, −1.50 to −1.99 as severely dry, and ≤−2.00 as extremely dry. The range and distribution of our SPI6 can be seen in the spline plots in Fig. 1*A*. Fig. S3 shows the monthly precipitation anomaly trends by country. The limited variability for Somalia (also visible in Fig. S5*F*) reflects the poorer data quality found in this area, especially during the last one-half of our study period; 5-y counts by grid cell of unusually dry months (SPI6 ≤ −1) are shown in Fig. S4*A*. There are relatively few dry months compared with the number of hot months during our study period (Fig. S4*B*), a phenomenon also visible in the SPI6 density distributions (Fig. 1). The first decade had substantially more dry periods than the succeeding 2000–2009 period.

Temperature. We use a 6-mo measure of temperature to quantify anomalies from the long-term climate record, because temperature trends have also been linked to civil war outbreaks (2), although this finding has been challenged (14). Global (6) and region-specific studies in China (15) and Europe (16, 17) support claims that rising and cooling temperatures will be associated with violence. Temperature variability has important implications for agriculture, and as such, this variable should be investigated with precipitation. In studies with different emphases (positive vs. negative temperature deviation), however, the mechanism remains the same: colder temperatures in temperate climates result in crop failure (18), and warmer deviations induce agricultural stress in warmer climates (19).

We use a 6-mo temperature index (TI6) to compare the current 6-mo mean temperature record with the long-term (since 1949) distribution for the same 6-mo period (see density plot of Fig. 1*B* for distribution). The calculation is similar to the SPI6, but it uses the standard normal distribution to parameterize the long-term distribution. The index expresses the 6-mo anomaly departure as an SD, enabling us to identify anomalous warm or cold periods. Fig. S3 shows the monthly temperature anomaly trends by country; 5-y counts of unusually hot months (TI6 ≥ 1) are shown in Fig. S4*B*, with the inland part of the East African study region experiencing the largest deviations in the 2000–2009 period.

c. Control variables—measures, data, and sources. Space–time lag. At international (20–23) and local levels (24–26), conflict exhibits qualities that might be described as contagion, diffusion, dependency, and clustering patterns. We account for these kinds of effects by including a space–time lag of the dependent variable. This space–time measure is constructed using a temporal lag of 1 mo and first-order spatial neighbors (queen contiguity) for the grids. Including the temporal lag removes the endogeneity problem of simultaneous spatial interaction that occurs with a pure spatially lagged regression model.

Population. Within a country, conflict risk is associated with greater population densities, numbers, and growth. We use the Gridded Population of the World (GPW; v3) data from the Center for International Earth Science Information Network and Socio-Economic Data and Applications Center of Columbia University (27). These data are available at multiple resolutions; we use the log-transformed 1° product for our independent variable and the finer resolution 2.5′ product to perform the population weighted calculations for other variables. The data are available for 5-y periods, and therefore, we estimate population values for intervening years using linear interpolation.

Wellbeing (infant mortality rate). We choose the infant mortality rate (IMR) as a summary measure of the overall quality of life in East African states; this indicator has also been used in previous studies of the climate–violence relationship (28). We use IMR instead of gross domestic product per capita, because it serves as a broader measure of social wellbeing. IMR is measured as the average number of deaths during the first 1 y of life per 1,000 live births. We assign IMR values to grid cells spanning country borders by weighting the IMR values based on GPW population data. IMR data are from the Interagency Group for Child Mortality Estimation, which is made up of representatives of the United Nations Children's Fund, World Health Organization, the World Bank, and the United Nations Population Division (29). Estimates for Somalia are static and high (at 108.3) between 1990 and 2008. All IMR values are lagged 1 y.

Political rights. In authoritarian political climates, violent social unrest may develop, because citizens have a limited ability to express their interests. We use the yearly political rights score from Freedom in the World 2011 (30) to measure the extent to which a society is autocratic or democratic in character. For grid cells spanning country borders, we assign the political rights value from the country with the most GPW population in the grid cell. It is generally accepted that regimes in transition between the two extreme categories experience the greatest risk of conflict. For each country and year, the political rights values range from one (free) to seven (not free). According to Freedom House (30), "[t]he ratings process is based on a checklist of 10 political rights questions (grouped into three subcategories). To answer the political rights questions, Freedom House considers to what extent the system offers voters the opportunity to choose freely from among candidates and to what extent the candidates are chosen independently of the state."

Presidential election. According to the work by Lindberg (31), only one-quarter of African elections can be considered peaceful. Violence may rise during campaigning or as a reaction to the outcome of an election (32, 33). To isolate the influence of this factor, we include a presidential election binary variable for every country. The value extends 3 mo before and 3 mo after a country's presidential poll. For grid cells spanning country borders, we assign the value from the country with the largest GPW population in the grid cell.

Ethnic leadership. Clientelism, patronage politics, or private rule is a known characteristic of political regimes in sub-Saharan Africa (34, 35). Patron–client ties can result in the (usually ethnic) exclusion of certain populations from government representation

and services (36, 37). We control for the fact that certain territories within states may benefit from central government patronage ties by developing a geographic representation of political leadership information from Archigos and Ethnologue spatial boundaries. We use the Archigos data (38) that contain the details of country leadership for 188 countries from 1875 to 2004. We updated the Archigos data from the available dataset using the existing coding protocol. A leader is defined as "the person that *de facto* exercised power in a country" (39). We focus on the dates of entry and exit from office. Also, the data outlining leadership of the study area countries were joined with a shapefile representation of traditional ethnic homelands developed from Ethnologue (40). For grid cells spanning an Ethnologue region, 20% or more of the grid area must be covered by the ethnicity of the country leader for it to assume the value of one.

Crop production index. There is a risk that social unrest will follow rising food prices because of unfavorable popular opinion and the fact that redressing food shortages adds pressure to strained government budgets by reducing expenditures elsewhere. As a surrogate for fluctuating food prices, we include a crop production index from the Food and Agriculture Organization and the World Bank (41). According to the World Bank, the "crop production index shows agricultural production for each year relative to the base period 1999–2001. It includes all crops except fodder crops. Regional and income group aggregates for the Food and Agriculture Organization's production indexes are calculated from the underlying values in international dollars, normalized to the base period 1999–2001" (41). We calculated percentage change from the previous year. Missing data for Ethiopia and Eritrea for the years 1990–1992 were estimated using a linear regression model based on crop production data for nonmissing years. For grid cells spanning country borders, we calculated a weighted average based on the respective GPW population.

Capital city. The capital city is frequently an important site of conflict (28), because it has symbolic importance (in terms of claiming control of a country at war); dominance there shows political control. It is also important to consider that lower-level skirmishes (e.g., protests) tend to cluster in a capital city, because it is the seat of important government offices. We use a binary measurement of whether a grid cell includes the capital city of a country. Asmara (Eritrea) was added starting in June of 1993 after that country gained independence.

Distance to border. Despite the efforts of state officials to secure and police their borders, international boundaries between African countries remain extremely porous. Because armed actors can use neighboring territory as a sanctuary, borders represent transmission points of conflict (26, 42). We calculate the mean distance to the international border for each grid cell based on a finer-resolution (10 km) distance grid. This finer-resolution distance grid was generated in ArcGIS using the Albers equal-area projection, and it was overlaid on the 1° grid to calculate the mean distance to the border. The mean distances were then converted to kilometers and transformed using the natural logarithm.

Distance to road. As routes for transporting people and supplies, roads are often a key target for military activity (43) while also serving as a key infrastructural element for central governments to attempt to maintain control over their territories (44). Although there are several options for mapping the road networks of East Africa, we found the road network data from the Digital Chart of the World (45) to be the most spatially consistent, and we selected primary and secondary roads from these data for our analysis. We use ArcGIS and the Albers equal-area projection to calculate the distance to roads for a finer-resolution (1 km) set of grids. These results are then overlaid on the 1° grid to calculate mean distance. The mean distances were then converted to kilometers and transformed using the natural logarithm.

Grassland. Pastoralist cattle raiding activity is a livelihood strategy in parts of our study area, especially northern Kenya (46). We account for the influence of this social dynamic by identifying pastoralist areas with a measurement of grassland land use from the History Database of the Global Environment database (47). We calculate the percent grassland by aggregating the 5′-resolution History Database of the Global Environment grassland area to our 1°-grid cells. Because the data are available only for 1990, 2000, and 2005, we perform a linear interpolation for intermediate years and extrapolate to 2009 by a linear extension of the 2000–2005 trends.

Vegetation condition index. We include a vegetation condition index (VCI) to control for variations in vegetation health over time. This weekly metric is derived from the National Oceanic and Atmospheric Administration's Advanced Very High Resolution Radiometer sensor (48). The vegetation condition index standardizes the normalized vegetation difference index (NDVI) to a range of 0–100 (Eq. **S1**):

$$\mathrm{VCI} = 100 \times (\mathrm{NDVI} - \mathrm{NDVI}_{\min}) / (\mathrm{NDVI}_{\max} - \mathrm{NDVI}_{\min}), \quad \textbf{[S1]}$$

where $\mathrm{NDVI}_{\min}$ and $\mathrm{NDVI}_{\max}$ values are the values per pixel (49–51). This index enables comparison of NDVI values across widely varying vegetation and precipitation regimens. These data are available weekly for the duration of the study period at 16-km pixel resolution from the National Oceanic and Atmospheric Administration's Center for Satellite Applications and Research. We aggregate them to our month grid unit of analysis by calculating the 4 wk mean value of all pixels within our 1° unit. Missing months from October to December of 1994 were filled using linear interpolation. We lag the VCI 6 mo with the expectation that any violence associated with changes in vegetation would not take place immediately. Our expectation is that declining vegetation health in the previous period is related to a decrease in food availability for both animals and humans and thus, increasing social and political stress.

Growing season. It is possible that the effect of temperature and precipitation deviations is greatest during growing seasons. A flood cannot destroy and a drought cannot desiccate crops that have not been planted. To test this effect, we include a binary variable for growing season derived from simulated climate data at a 10-arc min spatial resolution (49). Growing seasons were calculated based on average daily temperatures above 6 °C and a ratio of actual to potential evapotranspiration exceeding 0.35. These finer-resolution data were spatially aggregated to our 1° grids by averaging the start dates and end dates for each grid cell and then assigning the corresponding month based on the midpoints of each month.

II. Robustness Tests. To test the robustness of the relationships identified in the main regression model (Table 1, column f), we repeated this analysis using both spatial and temporal subsets of the data.

a. Country level. The first set of tests estimated model parameters for each of the nine core study area countries (Table S2). Because data for only one country at a time were included in the model, no country-level fixed effects were included (yearly fixed effects were retained). Additionally, for some of the countries, there was little to no variation in some of the country-scale variables. For instance, the ethnic leadership variable did not change during our study period for Burundi, Rwanda, and Somalia; this variable was, therefore, dropped from these country models. Similarly, Burundi, Eritrea, Ethiopia, and Rwanda had either one or no presidential elections between 1990 and 2009, and the election buffer variable was omitted for these country models. The political rights metric was dropped because of high collinearity with other explanatory variables for Burundi, Ethiopia, Somalia,

Tanzania, and Uganda. Similarly, the distance to road variable was dropped for Burundi because of collinearity.

The country-level estimates (Table S2) show wide fluctuations. Many control variables lose statistical significance, and other predictors shift from negative to positive significance between country models. Because N, the number of grid months, changes between the models, it is not possible to directly compare the log-likelihood and Akaike information criterion (AIC) values. To aid model comparison, we also report a pseudo-R^2 value (Nagelkerke R^2) and the area under the curve (AUC) for predictive capability. Precipitation and temperature spline plots for each country model show considerable differences between countries. SPI6 coefficients for Burundi, Kenya, Rwanda, Somalia, and Uganda are not statistically distinct from zero influence, although there is some evidence of a trend similar to the main generalized additive model (GAM) result, especially for wetter anomalies (Fig. S5). Results for Tanzania deviate from the general trend, a function of a peaceful and unique historical political trajectory compared with other countries. For temperature anomalies (Fig. S6), the overall relationship (Fig. 1*B*) holds up most consistently for Kenya, Ethiopia, and Somalia. For other country models, the results are not statistically different from zero, except for Burundi, where cooler than normal temperatures predict less conflict risk.

We experimented with dropping Somalia from the model, because the quality of political, social, and climate data was weaker for this country, which has seen ongoing civil wars during the full extent of our study period. The general trend for both the SPI6 and TI6 spline plots is similar to the main model (Fig. 1) after excluding Somalia, with no substantive interpretation differences. All coefficient estimates retain the same sign and level of significance as in the final model (Table 1, column f).

b. Five-year periods. We subset the data into four 5-y periods, with the caveat that the first 5-y period has only 4 y because of lagged variables omitting 1990. Model estimates for these four periods (Table S3, columns a–d) are slightly more stable than the individual country models, with fewer control variables oscillating between negative and positive coefficients. This stability is also evident in some of the precipitation and temperature spline plots. For SPI6, the periods 1995–1999 and 2000–2004 exhibit a similar pattern to the overall relationship (Fig. S7 *A–D*). The first and last time periods are not consistent with the overall model results, a result in line with the significance levels of splines in the tabular results. For TI6, portions of the overall relationship are evident in the results for all but the 1995–1999 5-y subset, with generally greater variability in the coefficient estimates (Fig. S8 *A–D*). The most recent period, 2005–2009, finds that cooler than normal temperatures are also associated with an increased risk of conflict.

c. Extreme climate conditions. We also test the effect of combined extreme weather conditions derived from our measures of precipitation and temperature. The hot and dry climate measure is a binary variable defined as one for TI6 ≥ 1 and SPI6 ≤ -1; otherwise, it is zero. Similarly, cold and wet grid months are defined for values of TI6 ≤ -1 and SPI6 ≥ 1. Results for these models (Table S3, columns e–f) show that hot and dry conditions as well as deviations that are both cold and wet have no influence on the risk of conflict. The addition of these measures has little impact on the spline plots for precipitation and temperature (Figs. S7 *E* and *F* and S8 *E* and *F*).

We also test the model for a subset of the data based on El Niño months. We define El Niño months using a 3-mo running mean of sea surface temperatures in the Niño 3.4 region (5° N to 5° S, 120° to 170° W) and a threshold of 0.5 °C warmer than the base period from 1971 to 2000 (52). This robustness test was inspired by the work by Hsiang et al. (6), which finds that the probability of conflict increases in El Niño years relative to La Niña years. We find the estimates for this model (Table S3, column g) to be roughly similar to the estimates of the overall model, with the effect of precipitation anomalies on conflict largely unchanged, although with a wider confidence interval for extreme precipitation anomalies (Fig. S7*G*). For temperature anomalies, warmer temperatures still predict an elevated risk of conflict, but for this El Niño subset, cooler temperatures also predict less conflict (Fig. S8*G*).

Because the East African climate is sensitive to sea surface temperature fluctuations in the Indian Ocean (52), we test how these fluctuations may influence conflict in an additional robustness check by including the Dipole Mode Index (DMI) in the model. The DMI is calculated by subtracting the sea surface temperature in the East Indian Ocean from the sea surface temperature in the West Indian Ocean for each month (53). The value is then assigned to each of the grid cells, and we tested models with the original DMI value and versions lagged for 3 and 4 mo. The 4-mo lag is most highly correlated with our SPI6 measure, and it also offered the strongest significant relationship with violence. Table S3, column h shows the coefficient estimates for this DMI robustness check; they are very similar to the main GAM model (Table 1, column f). The spline plots (Figs. S7*H* and S8*H*) are also similar to the spline plots in Fig. 1. From this robustness check, we conclude that the spatially invariant Indian Ocean sea surface temperature difference contributes little to the prediction of violence.

d. Alternative dependent variables and logit models. For this set of robustness tests, we use two different measures of localized conflict: a subset of the ACLED data and the UCDP data that are coded independently. We also vary the functional form of the model by truncating predicted values above one and substituting a logit model for the negative binomial model.

It is possible that weather variability and ecological stress will have the effect of increasing social unrest, such as riots or protests, and other types of informal conflict that do not include pitched battles between communal groups or between rebels and government forces. We selected the ACLED events that were coded as riots/protests and violence against civilians and recalibrated the model with only these events. The associations that we find between SPI6 and TI6 and conflict with this subset of data are similar to the full ACLED dataset (Table S4, column a). All controls retain the same sign as the full model, but our IMR measure for wellbeing becomes statistically significant. The greater effect of this variable may reflect a closer connection between riots and violence against civilians and wellbeing. The SPI6 spline coefficient estimates are nearly identical to our main model, with some dry anomalies predicting less violence (Fig. S9*A*). For this subset of data, like with the full model, conflict risk is greatest during months with high TI6 deviations from the long-term average (Fig. S10*A*).

We also modify the functional form of our main model with the full ACLED dataset (Table 1, column f) by truncating grid month violent event values greater than one and estimating the coefficients using a logistic generalized additive model. This approach helps to dampen the effect of high-intensity violence that might exert undue influence on the model estimates, although with the attendant disadvantage of reducing variation in the dataset. Results for this model (Table S4, column b) show general agreement with the negative binomial version, with no sign changes for any variables, although the political rights and crop production variables exhibit a stronger influence in predicting violence, whereas distance to road showed a reduced effect. The spline coefficient estimates for precipitation anomalies show a slightly reduced effect at warmer temperatures (Fig. S9*B*) but little change for temperature anomalies (Fig. S10*B*).

We also test the independently coded Georeferenced Event Dataset (GED) from UCDP. These data differ from our ACLED data primarily, because only records of deadly events of organized violence that take place within bouts of violence that killed at least 25 people in 1 y are included (54). This stricter definition means

that lower-intensity events, including conflict-related arsons, forced evictions, looting, rioting, and possibly other violent human injuries (all coded by ACLED), are excluded in the UCDP GED data. The UCDP GED data are currently available for all of Africa from 1989 to 2010 (55). In aggregating these point data to our grid month unit of analysis, we omitted events with temporal measure that was imprecise (e.g., a yearly indicator) and events with spatial precision that was only confirmed at the country or region/section scale. Several events with invalid dates were also omitted (e.g., February 31). For events coded as spanning many weeks, we elected to use the start day of the event rather than duplicating the event over the full date range, thus avoiding excessive counting for events. (Some cumulative events have a date range of longer than 1 mo, but this range usually relates to an ongoing political conflict rather than individual discrete instances of political violence that occurred on every day of that 1 mo.) Our modified file of the UCDP events, thus, yielded a total of 7,611 violent events for our nine-country study area from 1990 to 2009. Aggregated grid month UCDP counts are correlated positively with the ACLED data (Pearson's coefficient of 0.557).

The model estimates for UCDP GED violence are shown in Table S4, columns c and d. We use both the event count model and estimate a binary logistic response. When comparing ACLED with this more conservative definition of violence, the VCI is statistically significant, and the presidential election buffer is not significant in the event count negative binomial model. For the logistic model, capital city, political rights, and grassland are not statistically significant, whereas the vegetation index is statistically significant in the second model (not significant with the ACLED data). The spline estimates for precipitation anomalies (Fig. S9 *C* and *D*) show few differences from our main model. Results for temperature anomalies with the UCDP data are not statistically significant for the logit model, but they are significant for the negative binomial version (Fig. S10 *C* and *D*), with cooler temperatures predicting more violence and warmer temperatures predicting less violence.

e. Alternate independent variables. For this set of robustness checks, we consider variations of the independent variables. There is some debate about which controls are appropriate for the type of conflict analysis that we have conducted. Conceptually and empirically, there is strong justification to include possible effects of sociopolitical (e.g., regime type) and geographic (e.g., nearby conflict) realities. However, we test the effect of dropping all controls to eliminate the possibility that some of our ecological and physical geographical controls are associated with the key TI6 and SPI6 indicators (Table S4, column e). In doing so, both TI6 and SPI6 splines retain their statistical significance in this estimation, but the predictive power or fit of the model is lower without controls (AUC = 0.850 with controls and AUC = 0.723 without controls). In dropping all controls, the climate anomaly spline estimates vary little from our main model (Figs. S9*E* and S10*E*), supporting our expectation that the climate metrics are exogenous.

The neighboring violence control is a strong predictor of conflict and greatly increases the predictive power of our model. Dropping the space–time lag from our analysis generates results for both the TI6 and SPI6 indicators that are highly consistent with our initial findings (Figs. S9*F* and S10*F*). One exception is the reduced risk of conflict for the highest deviation dry periods. Given the dependence of violence over space and time, we believe that it is important to retain the space–time lag variable in our main model.

We also test for a relationship to the local growing season by a binary indicator of growing season status (Table S4, column g). These results show that growing season is not a statistically significant predictor of violence, and its inclusion does not affect the relationship of TI6 and SPI6 on conflict risk (Figs. S9*G* and S10*G*).

One explanation for the relationship between high temperature deviations and more conflict is that underrepresented, repressed, or politically excluded populations might suffer more under conditions of social stress and climate variability. We estimate four models, one for each of the following climate-related interaction terms: SPI6 × ethnic leadership, SPI6 × political rights, TI6 × ethnic leadership, and TI6 × political rights. None of these terms was statistically significant in predicting violence (Table S5, columns a–d). The climate variable spline plots for each model generally exhibit negligible differences with this interaction term included (Figs. S11 *A–D* and S12 *A–D*). The one exception is the precipitation anomaly plot for SPI6 interacted with political rights (Fig. S11*B*). For this model, the SPI6 and SPI6 × political rights terms have high generalized variance inflation factors, indicating a collinearity problem that manifests itself in the SPI6 spline plot. These results indicate that climate effects on conflict are independent of regime type and ethnic leadership as we have measured them.

To aid in coefficient interpretation, we also include a modified version of the hot temperatures binary model (Table 1, column d). In this modified model (Table S5, column g), we increase the TI6 binary threshold from 1 SD to 2 SDs. With this construction, we use the simpler generalized linear model composition in place of the more complex GAM model (Table 1, column f) to verify the effects of very hot temperatures on conflict. This additional model shows a very similar relative risk ratio for very hot grid months (a 30.2% increase compared with 29.6%, which is reported in Table 2). We also included the relative risk ratios for all coefficients in this model to facilitate comparison of climate effects to other factors. Presidential elections increase the risk of violence by a similar 35.1%, and presence of a capital city within a grid cell increases the risk of violence by a striking 511%. Note that the relative risk ratios may be easily calculated for any of our other negative binomial or logit models by exponentiating the reported coefficient. Caution is advised in comparing the magnitude of the coefficients and relative risk ratios directly; the input variable distributions are not standardized, and the ranges vary (Table S1).

f. Grid fixed effects and ordinary least squares functional form. Although we prefer country fixed effects for their ability to capture unmeasured institutional and governance variability at the country scale, we include models with grid (and year) fixed effects with and without control variables (Table S5, columns e and f). The stability of the climate anomaly spline plots (Figs. S11 *E* and *F* and S12 *E* and *F*) provides additional evidence that their effect on conflict is not sensitive to grid-level time invariant factors and that the climate variables are exogenous.

Because it is possible that the negative binomial functional form is inconsistent with large numbers of fixed effects for our models (ref. 56, p. 280), we also estimate the model using ordinary least squares (OLS). Table S6 mirrors the models of Table 1, except that it uses grid fixed effects instead of country fixed effects and estimates coefficients using OLS. Figs. S11*G* and S12*G* show the spline coefficient plots that correspond to Table S6, column f. These plots show that the effect of wet periods reducing conflict fades but that the effect of warmer temperatures increasing conflict remains.

1. Raleigh C, Linke A, Hegre H, Karlsen J (2010) Introducing ACLED: An armed conflict location and event dataset. *J Peace Res* 47:651–660.
2. Burke MB, Miguel E, Satyanath S, Dykema JA, Lobell DB (2009) Warming increases the risk of civil war in Africa. *Proc Natl Acad Sci USA* 106(49):20670–20674.
3. Singer J, Small M (1994) *Correlates of War Project: International and Civil War Data, 1816–1992*. Available at http://www.correlatesofwar.org/. Accessed June 19, 2011.
4. Gleditsch NP, Wallensteen P, Eriksson M, Sollenberg M, Strand H (2002) Armed conflict 1946–2001: A new dataset. *J Peace Res* 39:615–637.
5. Climate Change and Africa Political Stability (2011) *Social Conflict in Africa Database (SCAD)*. Available at http://strausscenter.org/scad.html. Accessed June 19, 2011.
6. Hsiang SM, Meng KC, Cane MA (2011) Civil conflicts are associated with the global climate. *Nature* 476(7361):438–441.

7. Benjaminsen TA, Alinon K, Buhaug H, Buseth JT (2012) Does climate change drive land-use conflicts in the Sahel? *J Peace Res* 49:97–111.
8. Raleigh C, Kniveton D (2012) Come rain or shine: An analysis of conflict and climate variability in East Africa. *J Peace Res* 49:51–64.
9. Theisen OM (2012) Climate clashes? Weather variability, land pressure, and organized violence in Kenya, 1989–2004. *J Peace Res* 49:81–96.
10. University of East Anglia (2011) *Climate Research Unit Database*. Available at http://badc.nerc.ac.uk/view/badc.nerc.ac.uk__ATOM__dataent_1256223773328276. Accessed May 6, 2011.
11. McKee TB, Doesken NJ, Kliest J (1993) The relationship of drought frequency and duration to time scales. *Proceedings of the Eighth Conference of Applied Climatology* (American Meteorological Society, Boston), pp 179–184.
12. Hayes M, Svoboda M, Wall N, Widhalm M (2011) The Lincoln declaration on drought indices: Universal meteorological drought index recommended. *Bull Am Meteorol Soc* 92:485–488.
13. Ntale HK, Gan TY (2003) Drought indices and their application to East Africa. *Int J Climatol* 23:1335–1357.
14. Buhaug H (2010) Climate not to blame for African civil wars. *Proc Natl Acad Sci USA* 107(38):16477–16482.
15. Zhang DD, et al. (2006) Climatic change, wars and dynastic cycles in China over the last millennium. *Clim Change* 76:459–477.
16. Tol RSJ, Wagner S (2010) Climate change and violent conflict in Europe over the last millennium. *Clim Change* 99:65–79.
17. Zhang DD, et al. (2011) The causality analysis of climate change and large-scale human crisis. *Proc Natl Acad Sci USA* 108(42):17296–17301.
18. Zhang DD, Brecke P, Lee HF, He Y-Q, Zhang J (2007) Global climate change, war, and population decline in recent human history. *Proc Natl Acad Sci USA* 104(49):19214–19219.
19. Lobell DB, Banziger M, Magorokosho C, Vivek B (2011) Nonlinear heat effects on African maize as evidenced by historical yield trials. *Nat Clim Chang* 13:42–45.
20. O'Loughlin J, Anselin L (1992) *The New Geopolitics*, ed Ward M (Gordon and Breach Science Publishers, Philadelphia), pp 11–38.
21. Anselin L, O'Loughlin J (1992) *The New Geopolitics*, ed Ward M (Gordon and Breach Science Publishers, Philadelphia), pp 39–76.
22. Houweling HW, Siccama JG (1985) The epidemiology of war, 1816–1980. *J Conflict Resolut* 29:641–663.
23. Siverson RM, Star H (1991) *The Diffusion of War: A Study of Opportunity and Willingness* (Univ of Michigan Press, Ann Arbor, MI).
24. Weidmann NB, Ward MD (2010) Predicting conflict in space and time. *J Conflict Resolut* 54:883–901.
25. O'Loughlin J, Witmer F (2011) The localized geographies of violence in the North Caucasus of Russia, 1999–2007. *Ann Assoc Am Geogr* 101:178–201.
26. Braithwaite A (2010) Resisting infection: How state capacity conditions conflict contagion. *J Peace Res* 47:311–319.
27. Center for International Earth Science Information Network (CEISIN) (2011) *Gridded Population of the World*. Available at http://sedac.ciesin.columbia.edu/gpw/index.jsp. Accessed October 25, 2011.
28. Theisen OM, Holterman H, Buhaug H (Winter 2011–2012) Drought, political exclusion, and civil war. *Int Secur* 36:79–106.
29. Interagency Group for Child Mortality Estimation (2011) *Infant Mortality Rate*. Available at http://childmortality.org. Accessed January 6, 2011.
30. Freedom House (2010) *Freedom in the World*. Available at http://freedomhouse.org. Accessed December 10, 2010.
31. Lindberg S (2006) *Democracy and Elections in Africa* (Johns Hopkins Univ Press, Baltimore).
32. Höglund K (2009) Electoral violence in conflict-ridden societies: Concepts, causes, and consequences. *Terrorism Polit Violence* 21:412–427.
33. Wilkinson SI (2004) *Votes and Violence: Electoral Competition and Ethnic Riots in India* (Cambridge Univ Press, New York).
34. Young C (1994) *The African Colonial State in Comparative Perspective* (BookCrafters, Chelsea, MI).
35. Rossler P (2011) The enemy within: Personal rule, coups, and civil war in Africa. *World Polit* 63:300–346.
36. Wucherpfennig J, Weidmann NB, Girardin L, Cederman L-E, Wimmer A (2011) Politically relevant ethnic groups across space and time: Introducing the GeoEPR dataset. *Conflict Manag Peace Sci* 10:1–15.
37. Wimmer A, Cederman L-E, Min B (2009) Ethnic politics and armed conflict. A configurational analysis of a new global dataset. *Am Sociol Rev* 74:316–337.
38. Goemans HE, Gleditsch KS, Chiozza G (2009) Introducing Archigos: A dataset of political leaders. *J Peace Res* 46:269–283. Available at http://rochester.edu/college/faculty/hgoemans/data.htm. Accessed October 3, 2011.
39. Goemans HE, Gleditsch KS, Chiozza G (2009) Introducing Archigos: A dataset of political leaders. *J Peace Res* 46:269–283.
40. World Language Mapping System (2010) *Ethnologue Global Spatial Representation of Ethnic Groups*. Available at http://worldgeodatasets.com/language/. Accessed May 29, 2010.
41. World Bank (2011) *Crop Production Index*. Available at http://data.worldbank.org/indicator/AG.PRD.CROP.XD. Accessed June 7, 2011.
42. Buhaug H, Gates S, Lujala P (2009) Geography, rebel capacity, and the duration of civil conflict. *J Conflict Resolut* 53:544–569.
43. Zhukov Y (2012) Roads and the diffusion of insurgent violence: The logistics of conflict in Russia's North Caucasus. *Polit Geogr* 31:144–156.
44. Herbst J (2000) *States and Power in Africa: Comparative Lessons in Authority and Control* (Princeton Univ Press, Princeton).
45. Danko D (1992) The digital chart of the world project. *Photogramm Eng Remote Sensing* 58:1125–1128.
46. Hendrickson D, Mearns R, Armon J (1996) Livestock raiding among the pastoral Turkana of Kenya: Redistribution, predation and the links to famine. *IDS Bull* 27:17–30.
47. Goldewijk KK, Beusen A, de Vos M, van Drecht G (2011) The HYDE 3.1 spatially explicit database of human induced land use change over the past 12,000 years. *Glob Ecol Biogeogr* 20:73–86.
48. National Oceanic and Atmospheric Administration (2011) *Advanced Very High Resolution Radiometer*. Available at http://www.star.nesdis.noaa.gov/smcd/emb/vci/VH/vh_ftp.php. Accessed June 8, 2011.
49. Jones PG, Thornton PK (2009) Croppers to livestock keepers: Livelihood transitions to 2050 in Africa due to climate change. *Environ Sci Policy* 12:427–437.
50. Singh RP, Roy S, Kogan F (2003) Vegetation and temperature condition indices from NOAA AVHRR data for drought monitoring over India. *Int J Remote Sens* 24:4393–4402.
51. Jiang L, et al. (2008) Adjusting for long term anomalous trends in NOAA's global vegetation index datasets. *IEEE Trans Geosci Rem Sens* 46:409–422.
52. National Oceanic and Atmospheric Administration (2011) National Weather Service Climate Prediction Center. Available at http://www.cpc.ncep.noaa.gov/products/analysis_monitoring/ensostuff/ensoyears.shtml. Accessed December 19, 2011.
53. Saji NH, Goswami BN, Vinayachandran PN, Yamagata T (1999) A dipole mode in the tropical Indian Ocean. *Nature* 401(6751):360–363.
54. Sundberg R, Lindgren M, Padskocimaite A (2010) *UCDP GED Codebook version 1.0-2011* (Department of Peace and Conflict Research, Uppsala University, Uppsala, Sweden).
55. Uppsala Conflict Data Program (UCDP) (2011) *Georeferenced Event Dataset*. Available at http://www.pcr.uu.se/research/ucdp/datasets/ucdp_ged/. Accessed December 11, 2011.
56. Cameron AC, Trivedi PK (1998) *Regression Analysis of Count Data* (Cambridge Univ Press, Cambridge, UK).

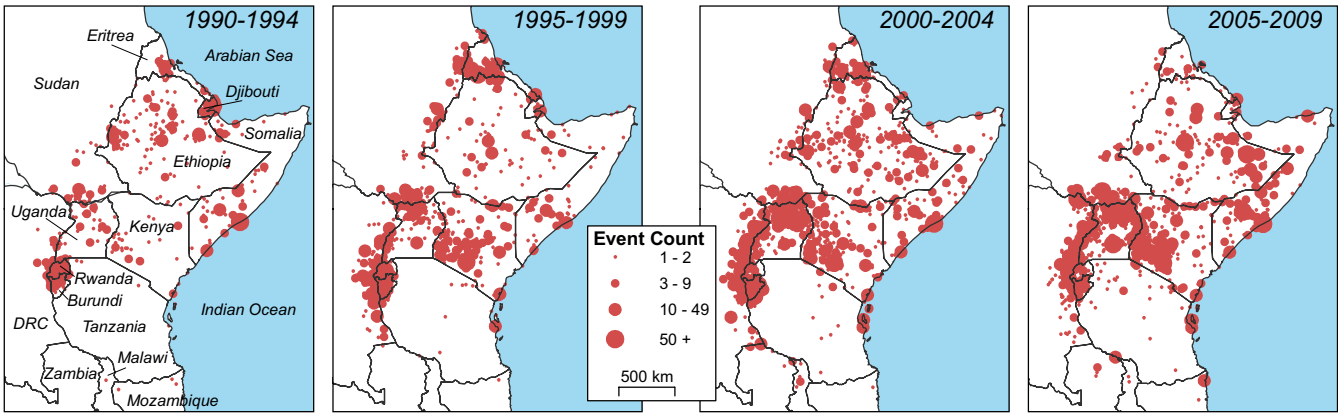

Fig. S1. The distribution of ACLED violent events for 5-y periods in the nine countries of the study area. The devastating civil conflicts in Rwanda (early 1990s) and Burundi (throughout the study period), the Ethiopia–Eritrea border war (1998–2000), the diffusion of violence into eastern Democratic Republic of Congo (DRC) from Rwanda, the Lord's Resistance Army war in northern Uganda and surroundings, the Ethiopian invasion of Somalia in mid-2006, the civil conflict in Somalia involving the Al-Shabab militias, and the Kenyan electoral violence of early 2008 are easily discernible on the maps. Border areas adjoining the nine countries of study (in Sudan, Zambia, DRC, Malawi, and Mozambique) are included in the analysis and have also seen violence.

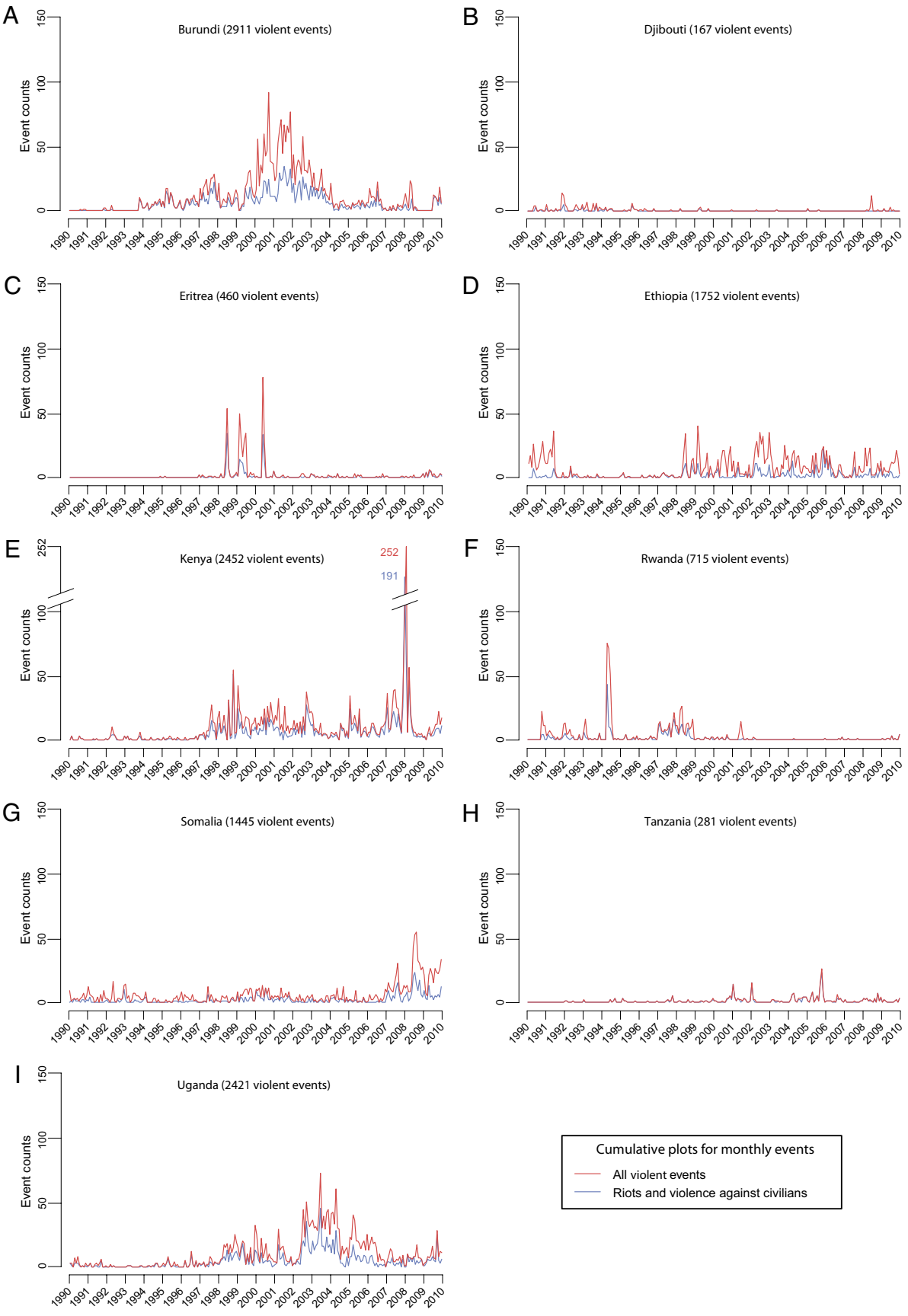

Fig. S2. Cumulative plots for ACLED monthly events by country.

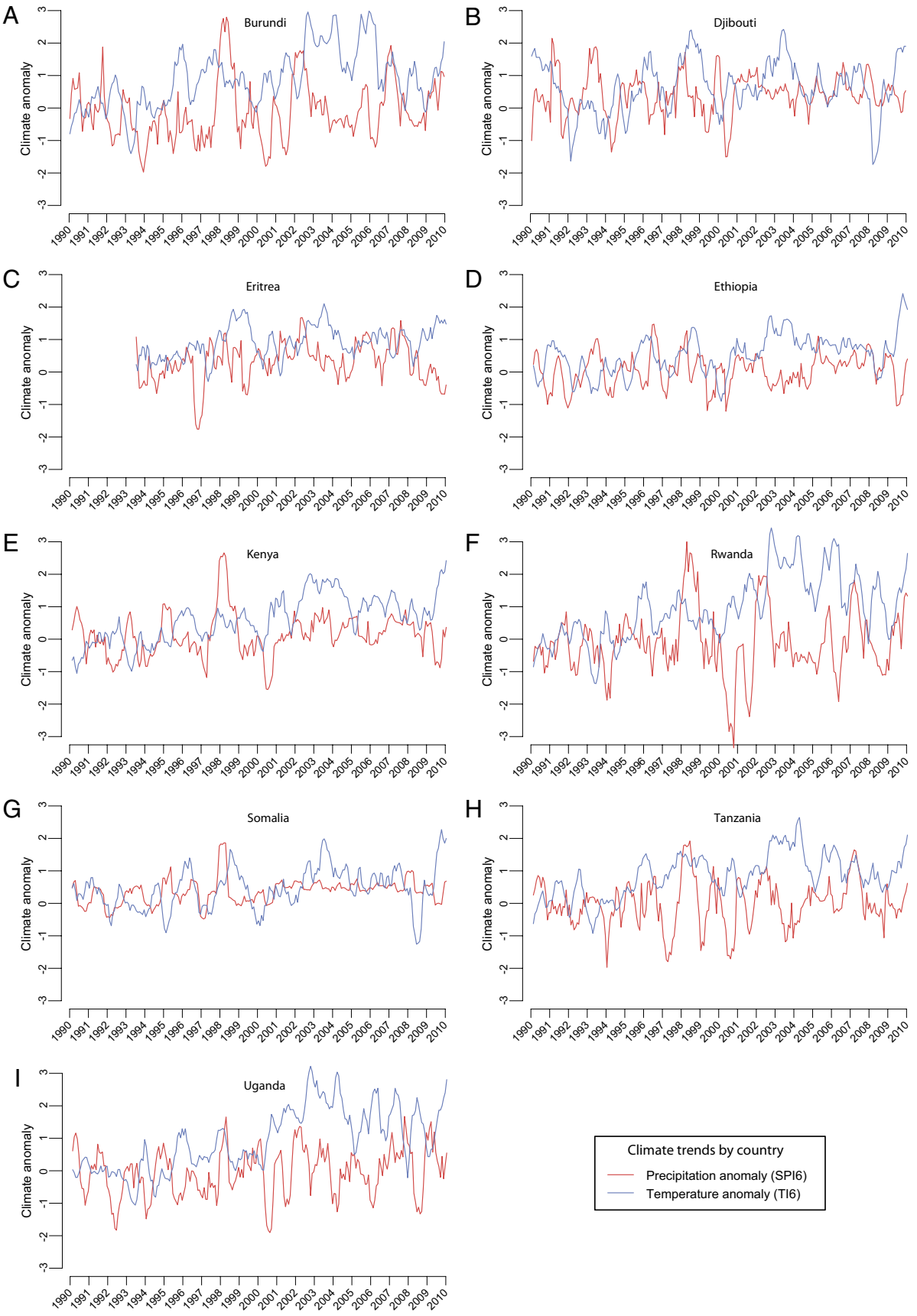

Fig. S3. Precipitation and temperature anomalies by country from 1990 to 2009.

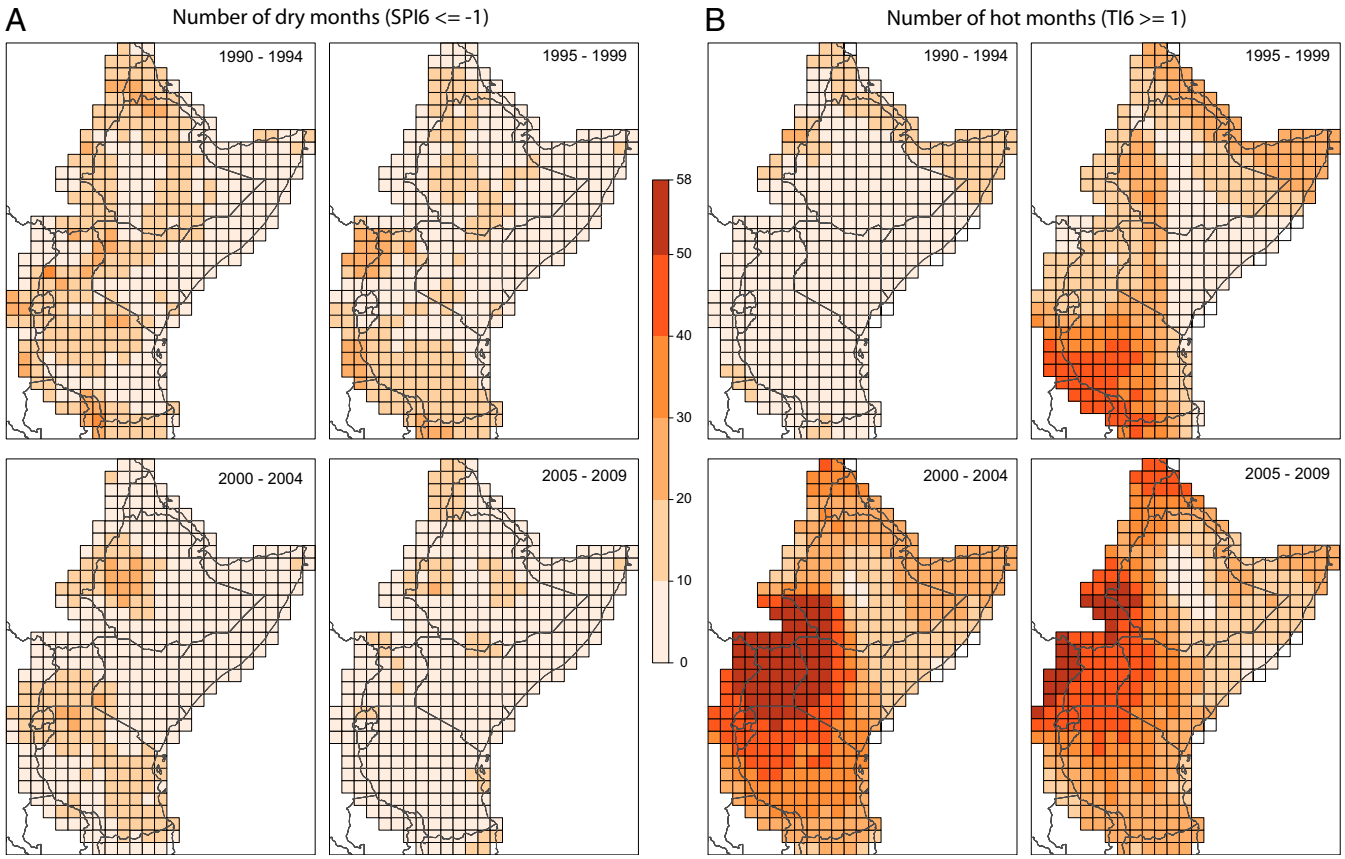

Fig. S4. Number of (*A*) dry and (*B*) hot months by 5-y period.

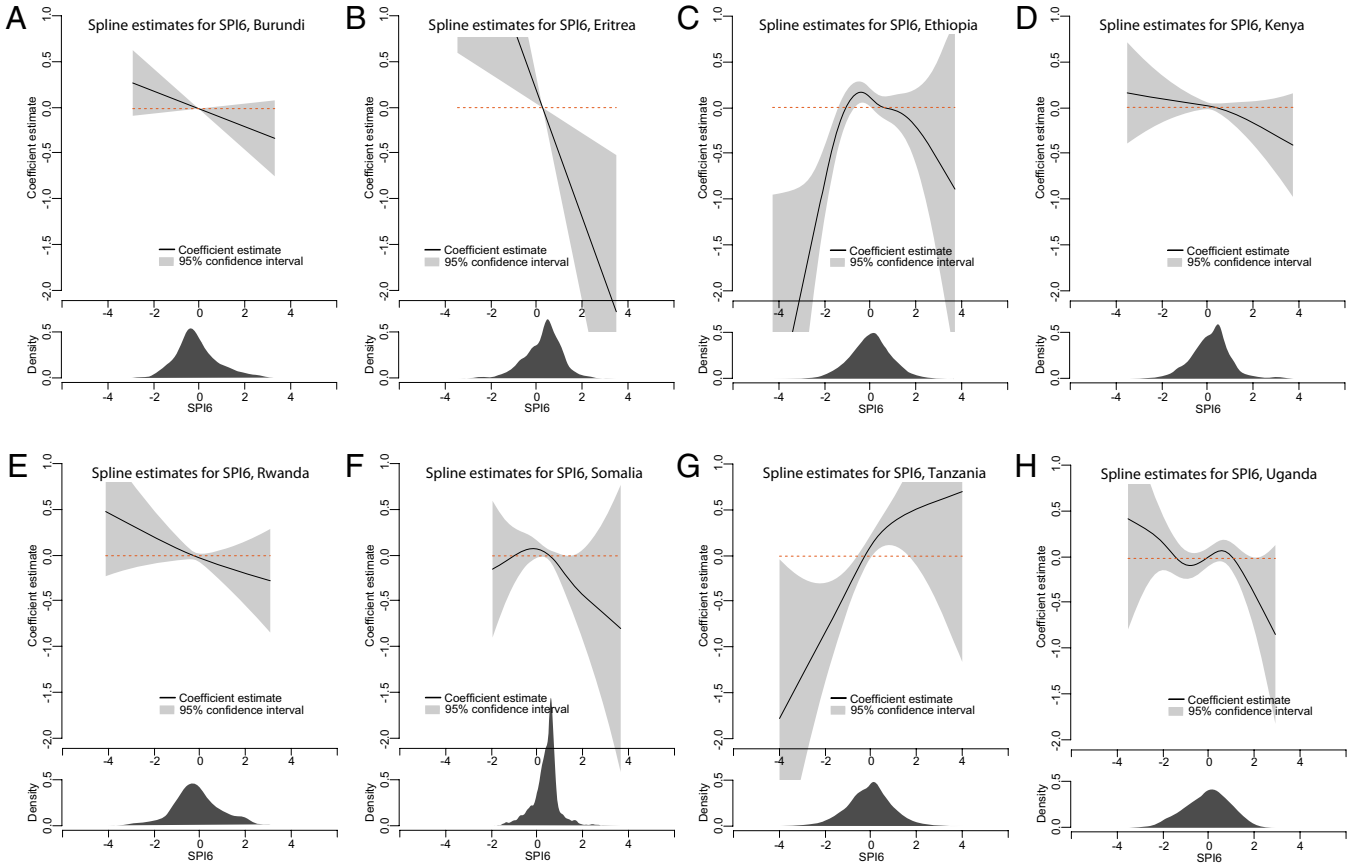

Fig. S5. Precipitation anomaly spline plots for country-level (*A*–*H*) robustness test subsets corresponding to Table S2, columns a–h.

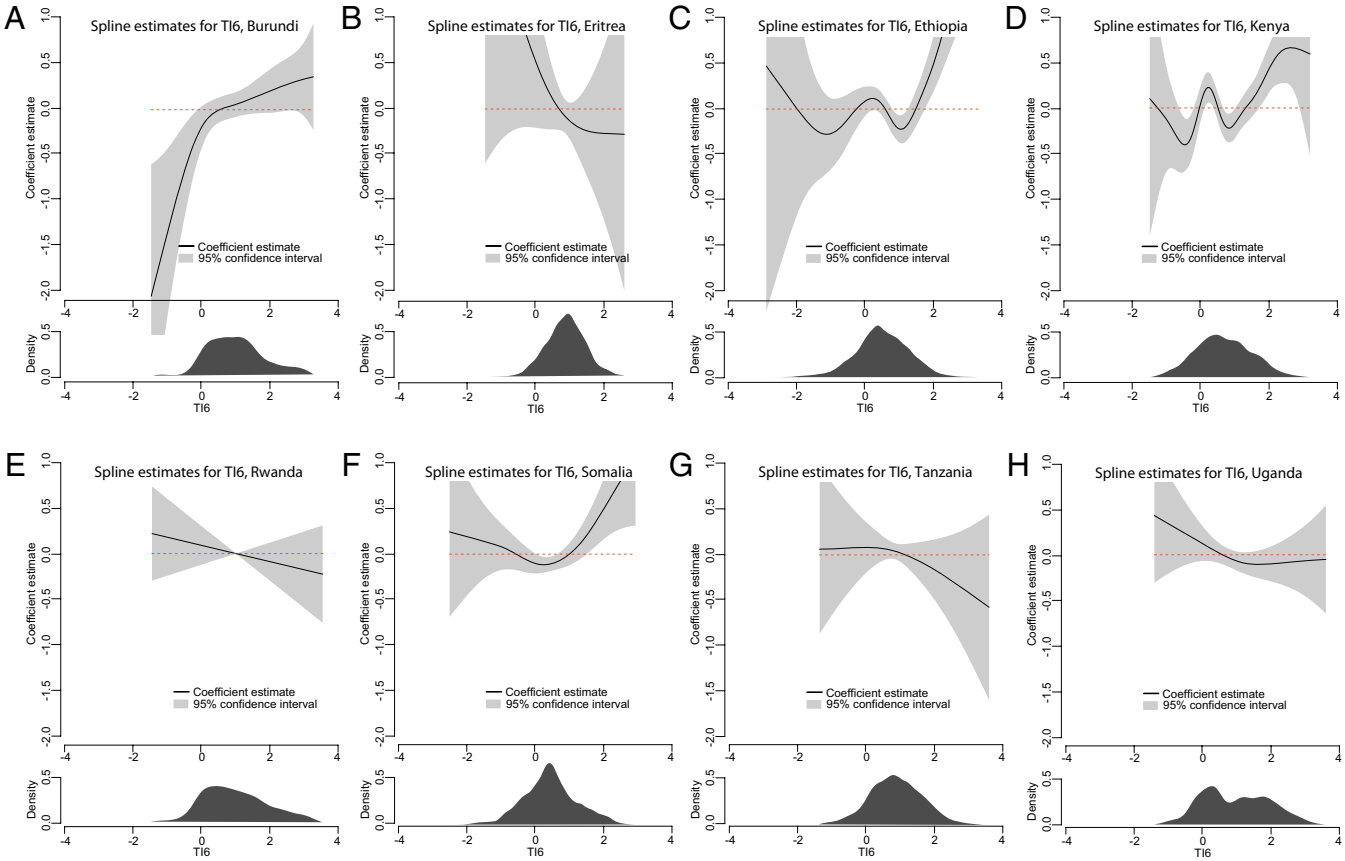

Fig. S6. Temperature anomaly spline plots for country-level (*A–H*) robustness test subsets corresponding to Table S2, columns a–h models.

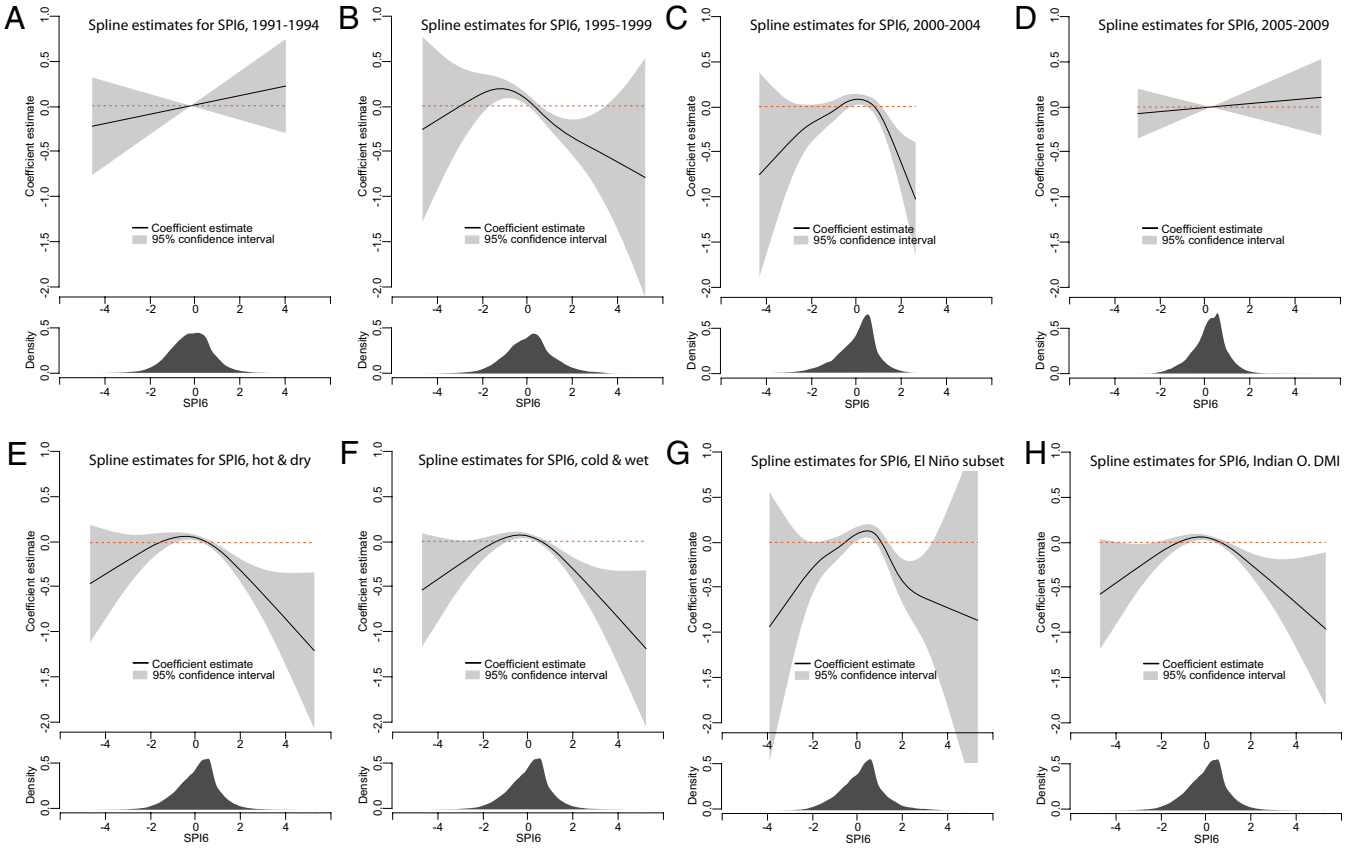

Fig. S7. Precipitation anomaly spline plots for 5-y periods (*A–D*), hot and dry (*E*), cold and wet (*F*), el Niño subset (*G*), and Indian Ocean DMI (*H*) corresponding to Table S3 models.

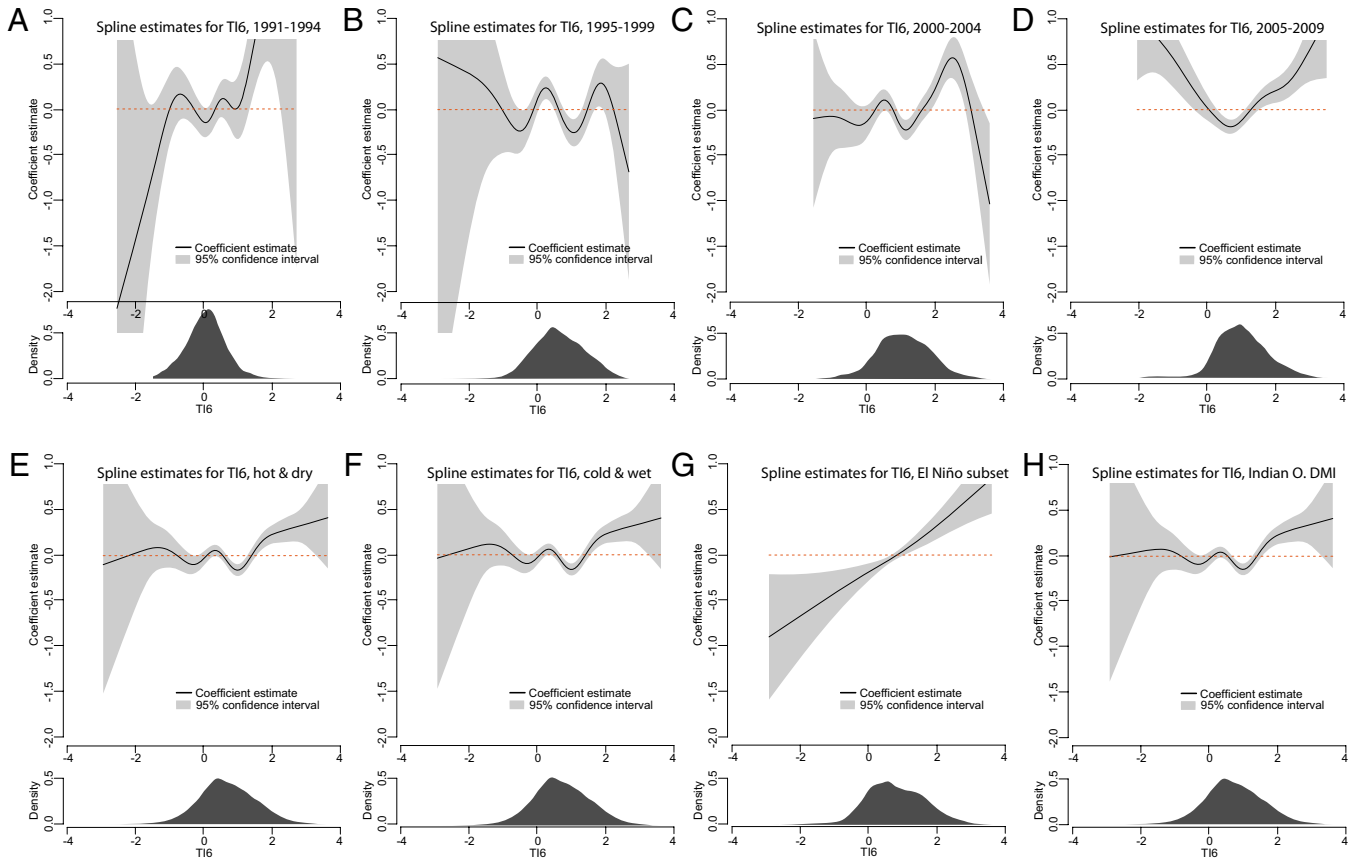

Fig. S8. Temperature anomaly spline plots for 5-y periods (*A*–*D*), hot and dry (*E*), cold and wet (*F*), El Niño subset (*G*), and Indian Ocean DMI (*H*) corresponding to Table S3 models.

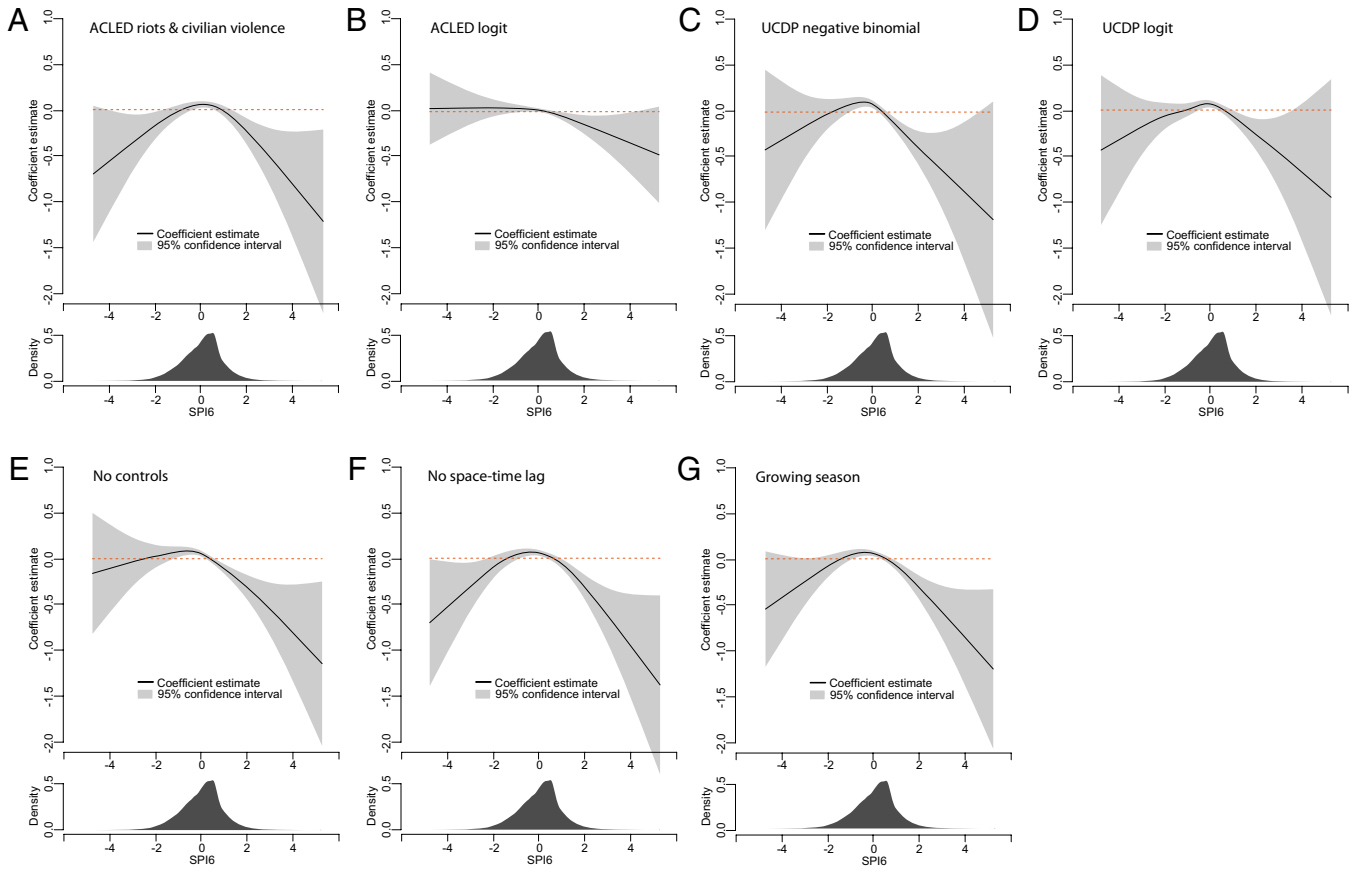

Fig. S9. Precipitation anomaly spline plots for alternate dependent variables and logit models (*A*–*D*) and alternate independent variables (*E*–*G*) corresponding to Table S4 models.

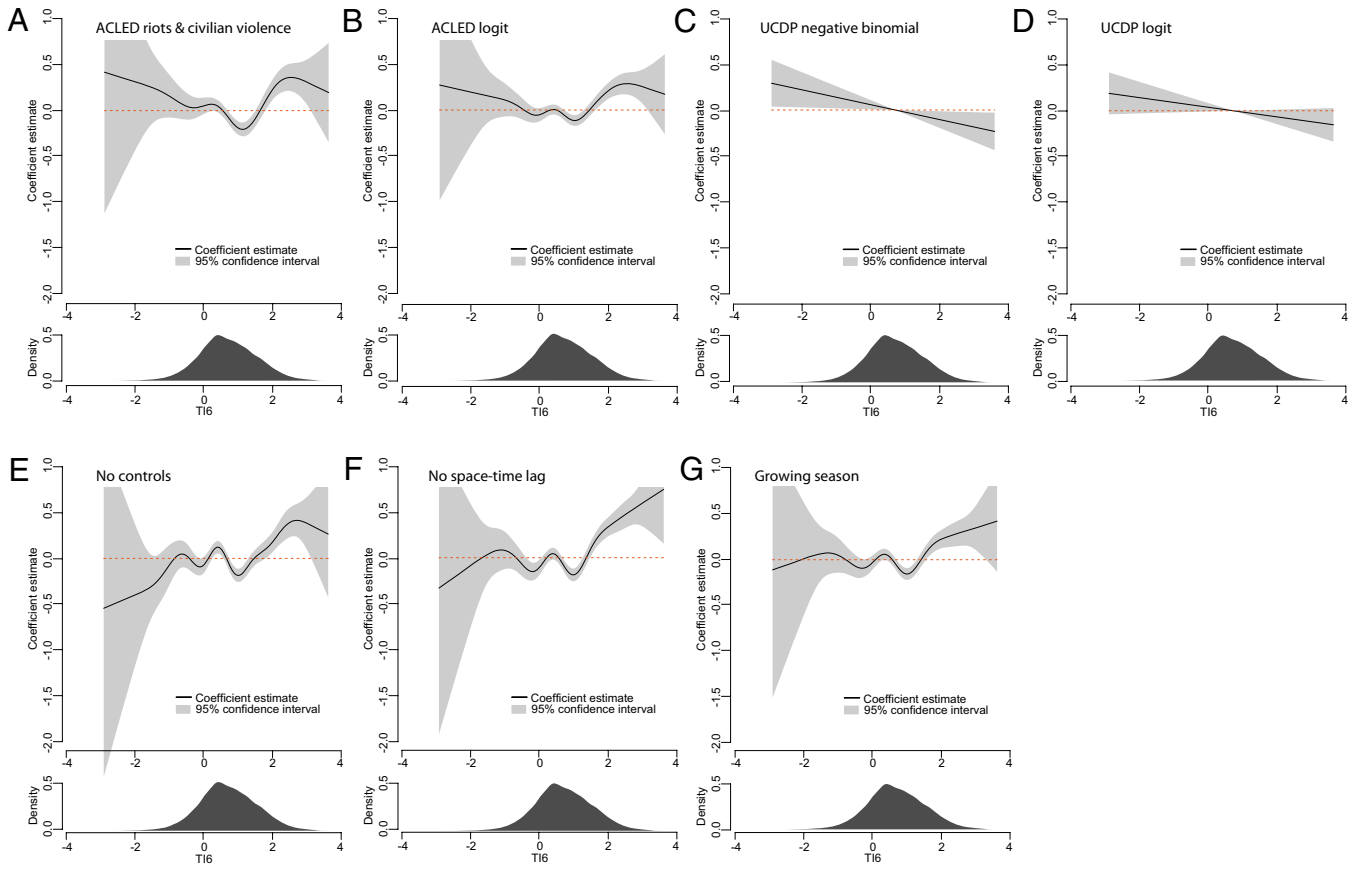

Fig. S10. Temperature anomaly spline plots for alternate dependent variables and logit models (*A*–*D*) and alternate independent variables (*E*–*G*) corresponding to Table S4 models.

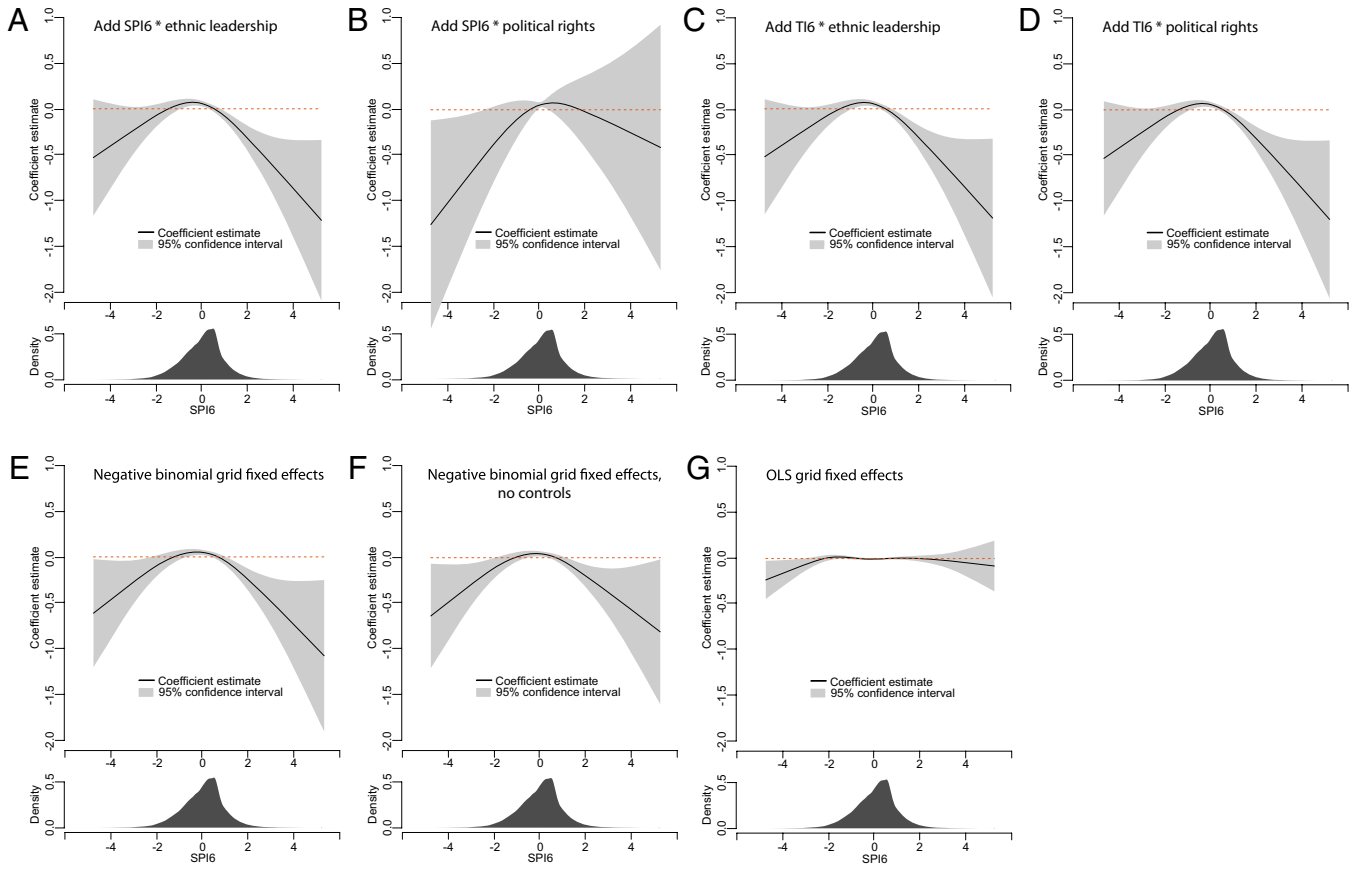

Fig. S11. Precipitation anomaly spline plots for interaction variables (*A*–*D*) and grid fixed effects (*E*–*G*) corresponding to models in Table S5, columns a–f, and Table S6, column f.

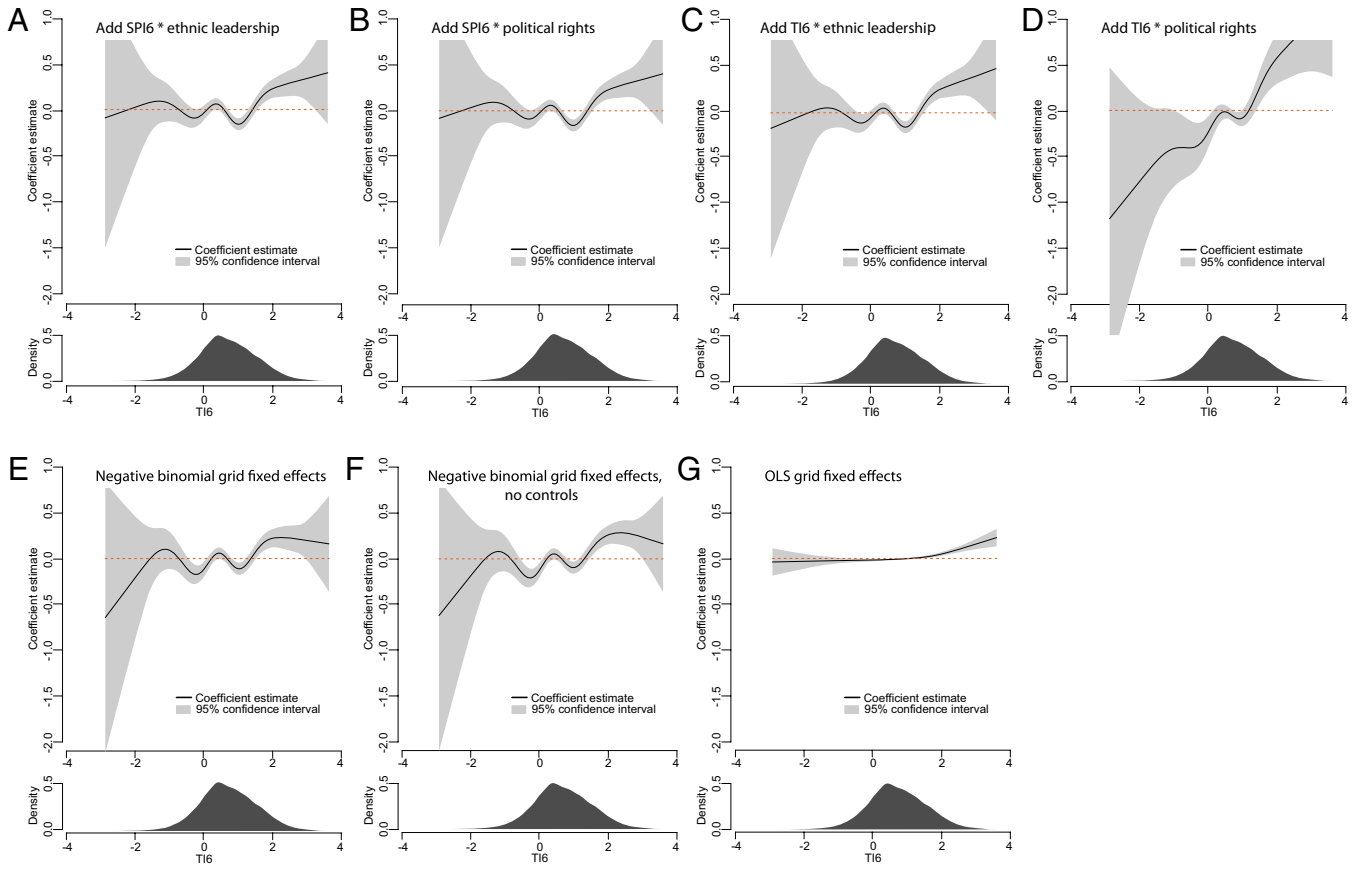

Fig. S12. Temperature anomaly spline plots for interaction variables (*A*–*D*) and grid fixed effects (*E*–*G*) corresponding to models in Table S5, columns a–f, and Table S6, column f.

Table S1. Summary statistics for dependent and independent variables

	Minimum	Median	Mean	Maximum	SD
ACLED violent events	0.000	0.000	0.175	53.000	1.275
UCDP violent events	0.000	0.000	0.080	43.000	0.746
Precipitation (SPI6)	−4.718	0.152	0.069	5.294	0.911
Temperature (TI6)	−2.909	0.670	0.710	3.619	0.823
Ethnic leadership	0.000	0.000	0.074	1.000	0.262
Distance to border (ln)	2.477	4.353	4.291	6.037	0.890
Capital city grid cell	0.000	0.000	0.022	1.000	0.147
Population (ln)	7.621	12.179	12.331	15.564	1.284
Wellbeing (IMR lag)	40.780	94.003	95.266	158.000	19.594
Political rights (lag)	2.000	6.000	5.492	7.000	1.234
Presidential election buffer	0.000	0.000	0.060	1.000	0.237
Grassland (%)	0.798	31.095	37.302	97.556	21.821
Distance to road (ln)	0.850	2.311	2.431	5.208	0.824
Crop production index (pct. Δ)	−35.484	1.499	3.257	104.000	12.816
VCI (lag)	0.000	48.840	48.461	100.000	21.680
Indian Ocean DMI (lag)	−2.735	−0.053	0.020	3.548	1.056
Growing season	0.000	0.000	0.403	1.000	0.490

Table S2. Negative binomial regression models for total number of violent events by country from 1991 to 2009

	a) Burundi		b) Djibouti		c) Eritrea		d) Ethiopia		e) Kenya		f) Rwanda		g) Somalia		h) Tanzania		i) Uganda	
	Estimate	*z* value	Estimate	*z* value	Estimate	*z* value	Estimate	*z* value	Estimate	*z* value	Estimate	*z* value	Estimate	*z* value	Estimate	*z* value	Estimate	*z* value
Intercept	−110.69	−1.599	−224.67	−2.905*	−164.27	0.000	−10.600	−3.174*	−0.975	−0.437	−263.10	−1.337	−12.690	−3.092*	−167.60	0.000	0.819	0.122
Space–time lag	0.052	1.881	−0.432	−1.057	0.100	1.099	0.460	5.471*	0.270	8.472*	0.213	7.410*	−0.189	−0.895	0.498	6.442*	0.347	9.867*
Spline (SPI6)	*P* value	0.118	*P* value	0.002*	*P* value	0.009*	*P* value	0.000*	*P* value	0.414	*P* value	0.176	*P* value	0.291	*P* value	0.004*	*P* value	0.118
Spline (TI6)	*P* value	0.052	*P* value	0.612	*P* value	0.245	*P* value	0.000*	*P* value	0.000*	*P* value	0.399	*P* value	0.012†	*P* value	0.328	*P* value	0.335
Ethnic leadership			−27.132	−2.954*	−1.709	−1.511	−0.456	−1.163	0.694	2.893*					−0.390	−1.163	−1.796	−3.696*
Distance to border (ln)	75.257	1.795	−0.637	−0.230	−0.064	−0.147	*P* value	−0.994	−0.223	−1.592	20.596	1.860	0.100	0.276	−0.534	−2.598*	0.832	2.002†
Capital city grid cell	−10.078	−2.232†	−11.393	−2.457†	−0.006	−0.009	2.453	8.222*	2.313	8.829*	3.683	0.829	1.734	3.307*	−0.161	−0.197	2.313	5.737*
Population (ln)	−7.530	−0.874	15.901	3.080*	0.973	2.629*	0.416	1.902	0.113	1.252	12.024	1.208	0.992	4.572*	1.788	3.672*	0.298	1.095
Wellbeing (IMR lag)	0.063	0.161	0.157	1.788	0.067	1.505	0.037	1.706	−0.024	−1.229	−0.010	−0.124	−0.035	−1.047	0.088	2.326†	−0.143	−4.184*
Political rights (lag)			−0.169	−1.116	2.342	3.046*			−0.187	−1.384	0.225	1.139						
Presidential election buffer			0.472	1.472					0.521	3.062*			−0.421	−1.147	0.754	1.548	0.573	3.236*
Grassland (%)	−0.670	−2.611*	−0.218	−2.383†	0.009	0.684	0.026	2.423†	−0.028	−1.971†	0.202	1.755	0.033	1.295	−0.018	−0.587	−0.003	−0.088
Distance to road (ln)			32.396	2.831*	−1.510	−2.426†	−0.760	−3.448*	−0.537	−2.312†	9.727	1.184	0.173	0.393	−0.421	−1.520	3.071	5.008*
Crop production index (pct. Δ)	−0.074	−4.211*	0.024	5.106*	0.000	−0.012	0.028	1.004	0.040	1.315	−0.121	−1.470	0.018	0.301	−0.010	−0.372	0.078	0.745
VCI (lag)	−0.002	−1.484	0.013	1.407	−0.005	−1.452	0.002	0.421	−0.004	−1.395	0.001	0.267	−0.003	−0.659	0.000	−0.061	−0.004	−0.956
Log-likelihood	−1,111.2		−336.0		−570.8		−4,100.0		−4,102.3		−1,299.9		−2,741.7		−814.1		−2,941.1	
AIC	2,285.7		738.0		1,202.9		8,275.7		8,283.8		2,662.1		5,550.8		1,694.5		5,952.4	
Nagelkerke R^2	0.958		0.499		0.523		0.294		0.452		0.475		0.539		0.592		0.464	
AUC	0.883		0.853		0.832		0.789		0.804		0.725		0.833		0.931		0.788	
N	684		912		2,388		21,096		11,400		912		13,908		18,012		3,876	

Variables were omitted because of no/little variation for the given country or severe collinearity problems.

*$P < 0.01$ using grid-clustered SEs.

†$P < 0.05$ using grid-clustered SEs.

Table S3. Negative binomial regression models for the total number of violent events by 5-y period and other climate robustness tests

	a) 1991–1994		b) 1995–1999		c) 2000–2004		d) 2005–2009		e) Hot and dry		f) Cold and wet		g) El Niño subset		h) Indian Ocean DMI	
	Estimate	*z* value	Estimate	*z* value	Estimate	*z* value	Estimate	*z* value	Estimate	*z* value	Estimate	*z* value	Estimate	*z* value	Estimate	*z* value
Intercept	−20.792	−5.826*	−6.945	−2.785*	−3.473	−1.845	−11.011	−4.897*	−8.300	−6.040*	−8.288	−6.026*	−10.020	−6.088*	−8.227	−5.976*
Space–time lag	0.326	4.494*	0.426	6.509*	0.432	9.533*	0.395	9.590*	0.514	14.814*	0.512	14.791*	0.449	7.499*	0.507	14.595*
Spline (SPI6)	*P* value	0.401	*P* value	0.000*	*P* value	0.001*	*P* value	0.606	*P* value	0.000*	*P* value	0.000*	*P* value	0.001*	*P* value	0.000*
Spline (TI6)	*P* value	0.008*	*P* value	0.000*	*P* value	0.000*	*P* value	0.000*	*P* value	0.000*	*P* value	0.000*	*P* value	0.000*	*P* value	0.000*
Ethnic leadership	−0.423	−1.488	−0.055	−0.164	−0.610	−2.447†	−0.426	−1.162	−0.332	−1.571	−0.332	−1.571	−0.218	−0.852	−0.335	−1.589
Distance to border (ln)	−0.359	−2.532†	−0.441	−3.545*	−0.419	−4.433*	−0.381	−3.444*	−0.417	−4.846*	−0.417	−4.845*	−0.378	−3.914*	−0.415	−4.813*
Capital city grid cell	1.048	3.543*	1.275	3.928*	1.563	4.988*	1.975	4.857*	1.626	5.654*	1.625	5.653*	1.674	6.640*	1.623	5.618*
Population (ln)	0.904	7.550*	0.604	7.215*	0.417	5.865*	0.498	5.303*	0.503	7.571*	0.502	7.547*	0.563	7.644*	0.504	7.559*
Wellbeing (IMR lag)	0.035	2.033†	−0.013	−0.871	−0.014	−1.224	0.043	2.970*	0.010	1.593	0.010	1.599	0.005	0.817	0.010	1.620
Political rights (lag)	0.553	2.233†	0.012	0.077	0.278	3.777*	−0.029	−0.174	0.092	1.905	0.092	1.893	0.167	2.861*	0.093	1.908
Presidential election buffer	0.032	0.096	0.163	0.566	0.154	0.780	0.612	4.299*	0.328	2.739*	0.325	2.715*	0.235	1.291	0.338	2.803*
Grassland (%)	0.034	4.272*	0.023	2.443†	0.017	2.573†	0.025	3.325*	0.020	4.086*	0.020	4.086*	0.023	4.021*	0.020	4.061*
Distance to road (ln)	−0.447	−2.380†	−0.296	−1.593	−0.369	−2.315†	−0.469	−3.054*	−0.387	−3.075*	−0.388	−3.084*	−0.318	−1.938	−0.390	−3.088*
Crop production index (pct. Δ)	−0.009	−2.569†	0.009	3.920*	−0.016	−3.002*	0.019	1.935	−0.004	−1.629	−0.004	−1.609	0.004	0.645	−0.004	−1.515
VCI (lag)	0.002	0.429	−0.002	−0.748	−0.001	−0.330	−0.002	−0.735	−0.002	−0.955	−0.002	−0.959	−0.003	−0.982	−0.002	−1.184
Hot and dry									−0.101	−0.857						
Cold and wet											0.334	−0.533				
Indian Ocean DMI (lag)															−0.103	−3.637*
Log-likelihood	−2,228.9		−5,687.6		−8,493.8		−8,193.4		−25,111.7		−25,111.5		−7,332.5		−25,102.1	
AIC	4,530.7		11,453.8		17,069.2		16,458.4		50,333.0		50,332.7		14,752.5		50,313.3	
Nagelkerke R^2	0.568		0.557		0.538		0.478		0.519		0.519		0.544		0.520	
AUC	0.876		0.877		0.830		0.833		0.850		0.850		0.863		0.850	
N	19,296		24,120		24,120		24,120		91,656		91,656		28,944		91,656	

Hot and dry is a binary variable defined for grid months with TI6 ≥ 1 and SPI6 ≤ −1; cold and wet grid months are defined similarly (TI6 ≤ −1 and SPI6 ≥ 1).

*$P < 0.01$ using grid-clustered SEs.

†$P < 0.05$ using grid-clustered SEs.

Table S4. Alternate dependent variables and logit models (a–d) and alternate independent variables (e–g)

	a) ACLED civilian/riot (events)		b) ACLED all events (logit)		c) UCDP negative (binomial)		d) UCDP logit		e) No controls		f) No space–time lag		g) Add growing season	
	Estimate	*z* value	Estimate	*z* value	Estimate	*z* value	Estimate	*z* value	Estimate	*z* value	Estimate	*z* value	Estimate	*z* value
Intercept	−10.503	−7.138*	−9.264	−6.804*	−4.137	−1.921	−7.302	−4.434*	−0.132	−0.194	−8.933	−6.099*	−8.312	−6.029*
Space–time lag	0.788	15.578*	0.736	11.130*	1.050	13.314*	1.318	15.945*	0.607	17.211*			0.511	14.696*
Spline (SPI6)	*P* value	0.001*	*P* value	0.036†	*P* value	0.000*	*P* value	0.006*	*P* value	0.000*	*P* value	0.000*	*P* value	0.000*
Spline (TI6)	*P* value	0.000*	*P* value	0.000*	*P* value	0.022†	*P* value	0.096	*P* value	0.000*	*P* value	0.000*	*P* value	0.000*
Ethnic leadership	−0.153	−0.710	−0.306	−1.444	−0.637	−1.621	−0.610	−1.661			−0.257	−1.161	−0.337	−1.591
Distance to border (ln)	−0.358	−4.462*	−0.362	−4.643*	−0.281	−2.052†	−0.272	−2.142†			−0.419	−4.808*	−0.417	−4.843*
Capital city grid cell	1.682	5.558*	1.423	3.518*	1.803	2.770*	0.983	1.715			1.451	4.841*	1.619	5.647*
Population (ln)	0.564	8.571*	0.503	7.199*	0.299	2.891*	0.332	3.660*			0.555	8.026*	0.507	7.573*
Wellbeing (IMR lag)	0.012	2.184†	0.010	1.893	−0.006	−0.682	0.005	0.697			0.013	2.051†	0.010	1.614
Political rights (lag)	0.034	0.711	0.121	2.766*	0.037	0.527	0.122	1.665			0.134	2.549†	0.092	1.894
Presidential election buffer	0.377	3.167*	0.277	3.045*	0.301	1.565	0.131	0.914			0.453	3.373*	0.336	2.797*
Grassland (%)	0.023	3.952*	0.022	4.596*	0.023	3.829*	0.023	3.715*			0.023	4.584*	0.020	4.063*
Distance to road (ln)	−0.407	−2.996*	−0.194	−1.648	−0.297	−1.976†	−0.044	−0.280			−0.346	−2.651*	−0.389	−3.076*
Crop production index (pct. Δ)	−0.003	−0.821	−0.005	−2.269*	−0.007	−1.794	−0.009	−2.504†			−0.007	−2.480*	−0.004	−1.607
VCI (lag)	0.001	0.299	−0.003	−1.806	−0.005	−2.039*	−0.005	−2.979*			−0.001	−0.755	−0.002	−0.993
Growing season													−0.096	−1.747
Log-likelihood	−15,321.6		−15,559.7		−14,593.9		−9,855.3		−26,768.3		−25,386.1		−25,108.5	
AIC	30,748.5		31,224.4		29,283.5		19,807.0		53,624.5		50,879.6		50,326.6	
Nagelkerke R^2	0.535		0.283		0.492		0.256		0.383		0.498		0.519	
AUC	0.878		0.852		0.849		0.857		0.802		0.844		0.850	

Number of observations for all models is 91,656 grid months. Models a, c, and e–g use the negative binomial functional form.

*$P < 0.01$ using grid-clustered SEs.

†$P < 0.05$ using grid-clustered SEs.

Table S5. Negative binomial regression models with interaction variables (a-d), grid fixed effects (e-f), and temperature binary (g)

	a) Add SPI6 × ethnic leadership		b) Add SPI6 × political rights		c) Add TI6 × ethnic leadership		d) Add TI6 × political rights		e) Grid and year fixed effects		f) Grid and year fixed effects (no controls)		g) TI6 binary (very hot; ≥ 2 σ)		
	Estimate	*z* value	Estimate	*z* value	Estimate	*z* value	Estimate	*z* value	Estimate	*z* value	Estimate	*z* value	Estimate	Relative risk	*z* value
Intercept	−8.283	−6.028*	−8.310	−6.043*	−8.283	−5.994*	−8.359	−6.080*	−66.625	−2.643*	−8,561.901	−1,063.265*	−8.209	0.000	−5.999*
Space–time lag	0.512	14.830*	0.511	14.783*	0.511	14.773*	0.513	14.749*	0.379	15.007*	0.399	16.000*	0.519	1.680	14.857*
Precipitation (SPI6)													−0.052	0.949	−1.648
Spline (SPI6)	*P* value	0.000*	*P* value	0.000*	*P* value	0.002*	*P* value	0.000*	*P* value	0.000*	*P* value	0.001*			
TI6 very hot													0.264	1.302	2.768*
Spline (TI6)	*P* value	0.000*	*P* value	0.000*	*P* value	0.000*	*P* value	0.000*	*P* value	0.000*	*P* value	0.000*			
Ethnic leadership	−0.333	−1.585	−0.331	−1.572	−0.145	−0.655	−0.341	−1.612	−0.055	−0.220			−0.320	0.726	−1.514
Distance to border (ln)	−0.417	−4.839*	−0.416	−4.838*	−0.418	−4.851*	−0.415	−4.820*	−0.664	−1.445			−0.422	0.656	−4.918*
Capital city grid cell	1.625	5.647*	1.626	5.645*	1.622	5.578*	1.624	5.646*	0.823	2.647*			1.631	5.111	5.666*
Population (ln)	0.502	7.558*	0.502	7.542*	0.504	7.564*	0.501	7.531*	−0.657	−1.141			0.495	1.641	7.479*
Wellbeing (IMR lag)	0.010	1.599	0.010	1.598	0.010	1.579	0.010	1.646	0.010	1.739			0.010	1.010	1.641
Political rights (lag)	0.092	1.890	0.095	1.983†	0.091	1.876	0.134	2.457†	0.070	1.583			0.085	1.088	1.732
Presidential election buffer	0.325	2.709*	0.324	2.707*	0.325	2.684*	0.333	2.771*	0.474	4.496*			0.301	1.351	2.519†
Grassland (%)	0.020	4.088*	0.020	4.095*	0.020	4.086*	0.020	4.085*	0.008	0.396			0.020	1.020	4.119*
Distance to road (ln)	−0.388	−3.084*	−0.389	−3.086*	−0.389	−3.088*	−0.393	−3.107*	9.548	1.382			−0.393	0.675	−3.116*
Crop production index (pct. Δ)	−0.004	−1.597	−0.004	−1.600	−0.004	−1.506	−0.004	−1.630	−0.004	−1.248			−0.004	0.996	−1.547
VCI (lag)	−0.002	−0.955	−0.002	−0.941	−0.002	−0.925	−0.001	−0.904	0.000	0.212			−0.002	0.998	−0.998
SPI6 × ethnic leadership	0.016	0.191													
SPI6 × political rights			0.132	−0.025											
TI6 × ethnic leadership					−0.198	−1.520									
TI6 × political rights							−0.048	−1.508							
Log-likelihood	−25,111.9		−25,110.9		−25,107.1		−25,108.7		−22,860.2		−22,904.8		−25,146.0		
AIC	50,333.6		50,331.5		50,324.0		50,327.3		46,603.0		46,672.0		50,385.9		
Nagelkerke R^2	0.519		0.519		0.519		0.519		0.655		0.653		0.517		
AUC	0.850		0.850		0.850		0.850		0.898		0.897		0.849		

Number of observations for all models is 91,656 grid months. Models a–d and g use country and year fixed effects.

*$P < 0.01$ using grid-clustered SEs.

†$P < 0.05$ using grid-clustered SEs.

Table S6. OLS regression models with grid and year fixed effects for total number of violent events per grid cell from 1991 to 2009

	a) Socioeconomic, physical, and climate		b) SPI6 binary dry (≤−1 σ)		c) SPI6 binary wet (≥1 σ)		d) TI6 binary hot (≥1 σ)		e) TI6 binary cold (≤−1 σ)		f) GAM splines	
	Estimate	*z* value	Estimate	*z* value	Estimate	*z* value	Estimate	*z* value	Estimate	*z* value	Estimate	*z* value
Intercept	0.053	0.029	0.045	0.025	0.054	0.030	−0.010	−0.006	−0.028	−0.015	0.441	0.294
Space–time lag	0.420	4.854*	0.420	4.855*	0.420	4.857*	0.422	4.859*	0.423	4.861*	0.419	5.935*
Precipitation (SPI6)	−0.001	−0.095					−0.003	−0.468	−0.004	−0.621		
SPI6 dry			0.015	0.668								
SPI6 wet					0.003	0.196						
Spline (SPI6)											*P* value	0.331
Temperature (TI6)	0.029	2.497†	0.029	2.482†	0.030	2.441†						
TI6 hot							0.022	1.772				
TI6 cold									−0.033	−1.309		
Spline (TI6)											*P* value	0.000*
Ethnic leadership	0.038	0.284	0.038	0.285	0.038	0.283	0.039	0.293	0.040	0.297	0.038	0.348
Distance to border (ln)	−0.155	−2.767*	−0.156	−2.797*	−0.155	−2.779*	−0.161	−2.846*	−0.157	−2.796*	−0.160	−3.495*
Capital city grid cell	−0.038	−0.285	−0.036	−0.271	−0.039	−0.286	−0.029	−0.221	−0.035	−0.258	−0.030	−0.280
Population (ln)	−0.003	−0.016	−0.001	−0.009	−0.003	−0.018	0.004	0.028	0.005	0.035	−0.002	−0.018
Wellbeing (IMR lag)	0.002	1.120	0.002	1.118	0.002	1.125	0.002	1.200	0.002	1.257	0.002	1.344
Political rights (lag)	0.027	1.759	0.027	1.761	0.027	1.765	0.028	1.781	0.028	1.787	0.027	2.172†
Presidential election buffer	0.054	1.297	0.054	1.315	0.054	1.272	0.056	1.352	0.058	1.395	0.053	1.553
Grassland (%)	0.006	1.272	0.006	1.271	0.006	1.274	0.006	1.286	0.006	1.288	0.005	1.536
Distance to road (ln)	−0.045	−0.691	−0.046	−0.716	−0.045	−0.687	−0.049	−0.764	−0.052	−0.815	−0.128	−3.398*
Crop production index (pct. Δ)	−0.001	−1.209	−0.001	−1.160	−0.001	−1.267	−0.001	−1.197	−0.001	−1.242	−0.001	−1.575
VCI (lag)	0.000	0.612	0.000	0.592	0.000	0.625	0.000	0.711	0.000	0.759	0.000	0.705
Log-likelihood	−139,429.8		−139,429.0		−139,429.8		−139,438.7		−139,440.7		−139,413.0	
AIC	279,727.6		279,726.0		279,727.5		279,745.5		279,749.4		279,706.6	
Nagelkerke R^2	0.410		0.410		0.410		0.410		0.410		0.410	
AUC	0.860		0.860		0.860		0.861		0.861		0.860	

Number of observations for all models is 91,656 grid months. Binary models b–d use precipitation and temperature anomalies of beyond 1 SD (σ) of the long-term mean to define the binary variable. Note that this table mirrors Table 1, except that it uses OLS as the functional form and grid fixed effects in place of country fixed effects.

*$P < 0.01$ using grid-clustered SEs.

†$P < 0.05$ using grid-clustered SEs.